

# Latest Triassic to Early Cretaceous tectonics of the Northern Andes: Geochronology, geochemistry, isotopic tracing, and thermochronology

Richard A. Spikings\*, Ryan Cochrane†, Cristian Vallejo‡, D. Villagomez\*, Roelant Van der Lelij§,  
A. Paul¶, Wilfried Winkler||

Department of Earth Sciences, University of Geneva, Geneva, Switzerland\* CRU, London, United Kingdom†  
Departamento de Geología, Facultad de Ingeniería en Geología y Petróleos, Escuela Politécnica Nacional, Quito,  
Ecuador‡ Norway Geological Survey, Trondheim, Norway§ School of Geosciences, The University of Edinburgh,  
Edinburgh, Scotland¶ Geological Institute, ETH Zürich, Zürich, Switzerland||

## 1 Introduction

The geological evolution of the western margin of northwestern Gondwana during the latest Triassic (209 Ma) to Early Cretaceous period is defined by a sudden change in tectonic style, compared to the preceding continental rift-to-drift setting and the early disassembly of Gondwana during 245–216 Ma (Cochrane et al., 2014a; Spikings et al., 2015). Continental Arc magmatism initiated at ~209 Ma, and was temporally continuous until the margin was temporarily disrupted by the collision and accretion of the Caribbean Large Igneous Province at ~75 Ma. This manuscript is a review of the latest Triassic-Early Cretaceous history of the Northern Andes (north of 5°S) with an emphasis on the evidence provided by crystalline rocks. We combine accurate geochronology (zircon U-Pb), geochemistry (major oxides, trace and REE), isotopic tracing (Hf, Sr, Nd, Pb), high-temperature (>350°C) thermochronology, and field observations with the geochronology of detrital zircons to construct a coherent tectonic model. These data were collected from rocks that have been considered to represent exotic continental terranes, or oceanic arcs (e.g., the Alao and Quebradagrande Arcs; see Litherland et al., 1994; Toussaint and Restrepo, 1994), although Pratt et al. (2005), Cochrane et al. (2014b), and Spikings et al. (2015) recently argued that they are para-autochthonous to South American crust.

The latest Triassic-Cretaceous (>115 Ma) period was characterized by arc magmatism that formed during a prevailing extensional regime. Prolonged extension formed an arc axis that migrated oceanward, and formed on lithosphere that was progressively thinning, constructing more geochemically primitive and isotopically juvenile arcs. Extension was sufficient in some locations to generate transitional-MOR

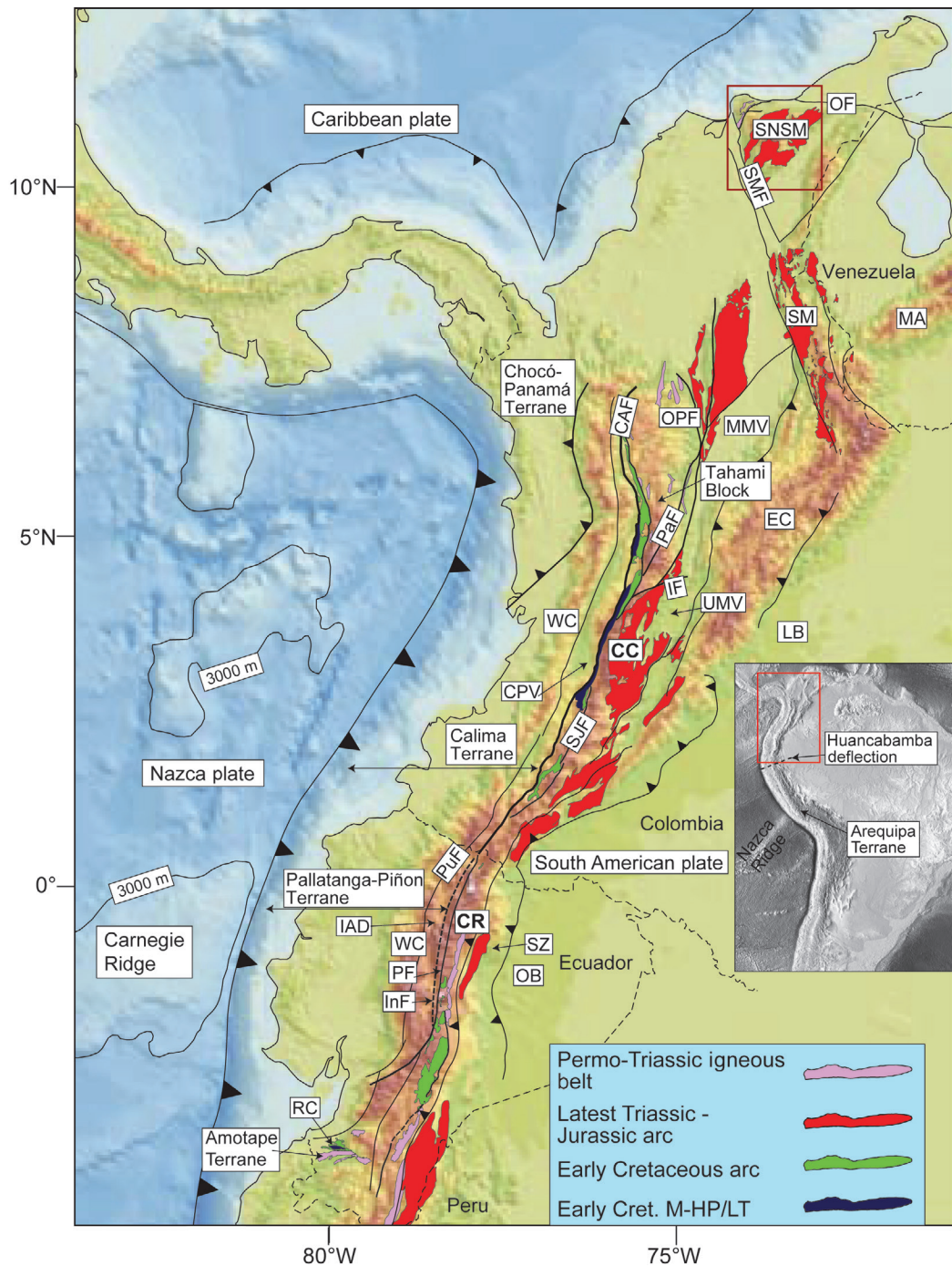
crust that was dominated by isotopically juvenile mafic and ultramafic rocks. We argue that compression occurred at ~115 Ma, resulting in the exhumation and obduction of HP-LT metamorphic assemblages onto the western arc flank, and closure of marginal basins that formed during prior extension. [Collins et al. \(2011\)](#) refer to contiguous extension and compression along an active margin as switching tectonics, which has important implications for the mechanisms of destruction and creation of new continental crust as the asthenosphere cycles between tectonic exhumation and burial.

## 2 Geological framework

A majority of the rocks exposed in the Northern Andes (north of 5°S) formed as a consequence of subduction of Pacific oceanic lithosphere beneath continental crust of north-western South America. Subduction has been almost continuous since ~209 Ma ([Litherland et al., 1994](#); [Spikings et al., 2015](#)), although it has been interrupted by changing rollback velocities, changing plate convergence vectors and terrane accretion ([Aspden et al., 1987](#); [Bayona et al., 2006](#); [Pindell and Kennan, 2009](#); [Villagomez et al., 2011](#); [Cochrane et al., 2014a](#); [Spikings et al., 2015](#)).

The metamorphic Paleozoic-Triassic basement of the Eastern Cordillera of Ecuador and Central Cordillera of Colombia ([Fig. 1](#)), which expose equivalent rocks sequences ([Figs. 2 and 3](#)), was intruded by an I-type, calc-alkaline continental arc between ~209 and 145 Ma ([Litherland et al., 1994](#); [Villagomez et al., 2011](#); [Cochrane et al., 2014b](#); [Spikings et al., 2015](#); [Bustamante et al., 2016](#); [Leal-Mejía et al., 2018](#); [Rodriguez et al., 2018](#)). Within Ecuador, these batholiths are called the Rosa Florida, Abitagua, and Zamora batholiths, which are located along the eastern flank of the Eastern Cordillera. Jurassic volcanic arc rocks are grouped within the Misahualli Formation ([Litherland et al., 1994](#); [Pratt et al., 2005](#)), which is mainly exposed in the proximal retroforeland, and thus they are not shown in [Figs. 2 and 3](#). Similar Jurassic-aged batholiths within the Central Cordillera of Colombia include, among others (see compilation in [Leal-Mejía et al., 2018](#)), the Ibagué, Segovia, and San Lucas batholiths, isolated plutons along the eastern and western flanks of the Upper Magdalena Valley ([Rodriguez et al., 2018](#)), and volcanic rock sequences within the Saldaña and Noreán formations (e.g., [Vinasco et al., 2006](#)). Jurassic intrusions also crop out in the Sierra Nevada de Santa Marta ([Figs. 1 and 4](#)) where tonalities are also common ([Alvarez, 1983](#); [Colmenares, 2007](#)), and latest Triassic-early Jurassic plutons are abundant in the Santander Massif ([Figs. 2 and 3](#); Santander Plutonic Group), with associated volcanic rocks of the Guatapurí Fm. The intrusive rocks are generally dominated by coarse, biotite quartz monzonites, monzogranites and hornblende-biotite granites, granodiorites and minor diorites, and are usually undeformed.

Traversing oceanward (westward) from the Jurassic batholiths and crossing the mylonites and ultramylonites of the Cosanga Fault in Ecuador ([Fig. 2](#)), the relict Salado basin, which is now deformed within the Cordillera Real is characterized by interbedded Upper Jurassic - Lower Cretaceous turbiditic metasedimentary rocks and mafic lavas (Upano Unit). These are in faulted or unconformable contact with the foliated, I-type calc-alkaline Azafrán Batholith (145–140 Ma; [Figs. 2 and 3](#); [Spikings et al., 2015](#)). Similar rock sequences are found in the Cordillera Central, and intrusive rocks of the Mariquita Stock ([Figs. 2 and 3](#); [Bustamante et al., 2016](#)) are probably equivalent to the Azafrán Batholith (similar ages and composition; see [Sections 3 and 4](#)). [Ballock \(1982\)](#), [Pratt et al. \(2005\)](#) and [Spikings et al. \(2015\)](#) suggest the metasedimentary rocks, such as those in the relict Salado Basin, are equivalent to Cretaceous sedimentary rocks (Hollin and Napo fms.) that are exposed within the region of the Amazon

**FIG. 1**

See figure caption on next page.

Foreland Basin (Fig. 1), and formed in a margin setting. However, Litherland et al. (1994) regard the Upano Unit as having a distinctly different history based on their metamorphic grade, and assign them, along with the Azafrán Batholith, to the fault bounded “Salado” Terrane.

Continuing westwards within the Cordillera Real, the Upano Unit is faulted against (Llanganates Fault; Figs. 2 and 3) poorly differentiated Paleozoic metasedimentary rocks and Triassic anatectites (Litherland et al., 1994; Cochrane et al., 2014b; Spikings et al., 2015). Pratt et al. (2005) interpret this contact as either a metamorphosed intrusive contact or an unconformity. Further west, these are faulted against greenschist grade para-graphitic schists, and submarine meta-andesites and meta-agglomerates of the Alao Arc, across the Baños Fault (Figs. 2 and 3). The few geochronological determinations of the Alao Arc include K/Ar dates of volcanic rocks (Herbert and Pichler, 1983; Litherland et al., 1994), U-Pb dates of detrital zircons (Cochrane et al., 2014b; Spikings et al., 2015), and Jurassic pollen, spores, and acritarchs (Riding, 1989). Numerous unsuccessful attempts have been made by the current authors to extract zircons from the most differentiated mafic igneous rocks of the Alao Arc. Bristow (1973) considered these lithologies to be equivalent to sedimentary rocks that are now exposed within the Western Cordillera of Ecuador (Yunguilla Fm.). Litherland et al. (1994) interpret these to represent a distinct island arc terrane, which they refer to as the Alao Arc, while Spikings et al. (2015) interpret these as an arc that formed on attenuated continental crust. The western margin of these sequences is defined by the 1–2 km wide Peltetec fault zone (PF in Fig. 1), which hosts inliers of steeply dipping, anastomosed blocks of peridotite, olivine gabbros, spilitized dolerites, basalt and volcanoclastic rocks. Litherland et al. (1994) interpret these to define an ophiolitic assemblage, which they refer to as the Peltetec Unit, and Spikings et al. (2015) show that they crystallized at ~135 Ma within a hyperextended basin. Pratt et al. (2005) describe a stratigraphic transition from the greenschists of the Alao Arc into metasedimentary rocks located west of the Peltetec Unit, and thus they rule out the Peltetec Fault as a terrane boundary. Finally, the Peltetec Unit defines the eastern boundary of a series of gently dipping slates and quartzites, which are exposed in isolated inliers, and host Jurassic-Early Cretaceous ammonites. Litherland et al. (1994) named these the “Guamote Sequence” and suggest they form part of allochthonous continental crust of the Chaucha Terrane (represented by the Guamote sequence in Fig. 2), whereas Pratt et al. (2005) and Spikings et al. (2015) suggest they are equivalent to sedimentary rocks exposed in the Alao volcanic sequence. The same sequence of rocks is exposed with the Amotape Terrane of southern Ecuador (Figs. 1 and 2), which is rotated ~65° clockwise relative to the Cordillera Real. Here, the Triassic anatectites are faulted against a complicated mélange of deformed and metamorphosed igneous rocks that are considered to represent an accretionary prism. The mélange hosts

#### FIG. 1, CONT'D

Digital elevation model for northwestern South America showing the cordilleras, terranes, main faults, and the exposure of Permian-Cretaceous magmatic rocks in Ecuador and Colombia. Small red box indicates the location of Fig. 3. Inset shows the location of the Arequipa Terrane in southern Peru. Faults: CAF, Cauca-Almaguer Fault; IF, Ibagué Fault; Inf, Ingapirca Fault; OF, Oca Fault; OPF, Otu-Pericos Fault; PaF, Palestina Fault; PF, Peltetec Fault; PuF, Pujili Fault; SJF, San-Jeronimo Fault; SMF, Santa Marta Fault. Other abbreviations: CC, Cordillera Central; CPV, Cauca-Patía Valley; CR, Cordillera Real; IAD, Interandean Depression; LB, Llanos Basin; MA, Merida Andes; MMV, Middle Magdalena Valley Basin; OB, Oriente Basin; RC, Raspas Complex; SM, Santander Massif; SNSM, Sierra Nevada de Santa Marta; SZ, Sub-Andean Zone; UMV, Upper Magdalena Valley Basin; WC, Western Cordillera. Geology from Litherland et al. (1994) and Gomez et al. (2007).

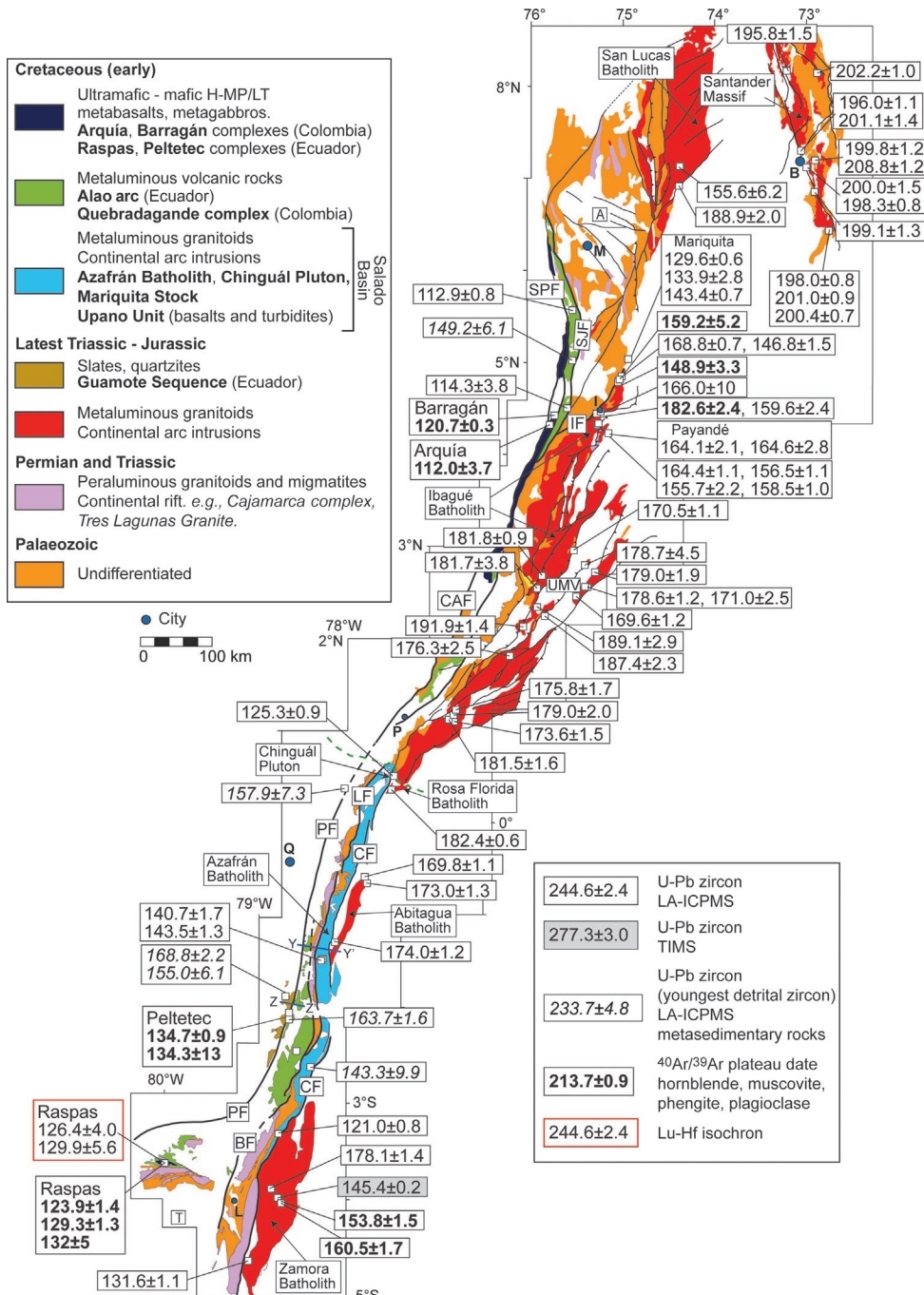


**FIG. 2**

---

See figure caption on next page.

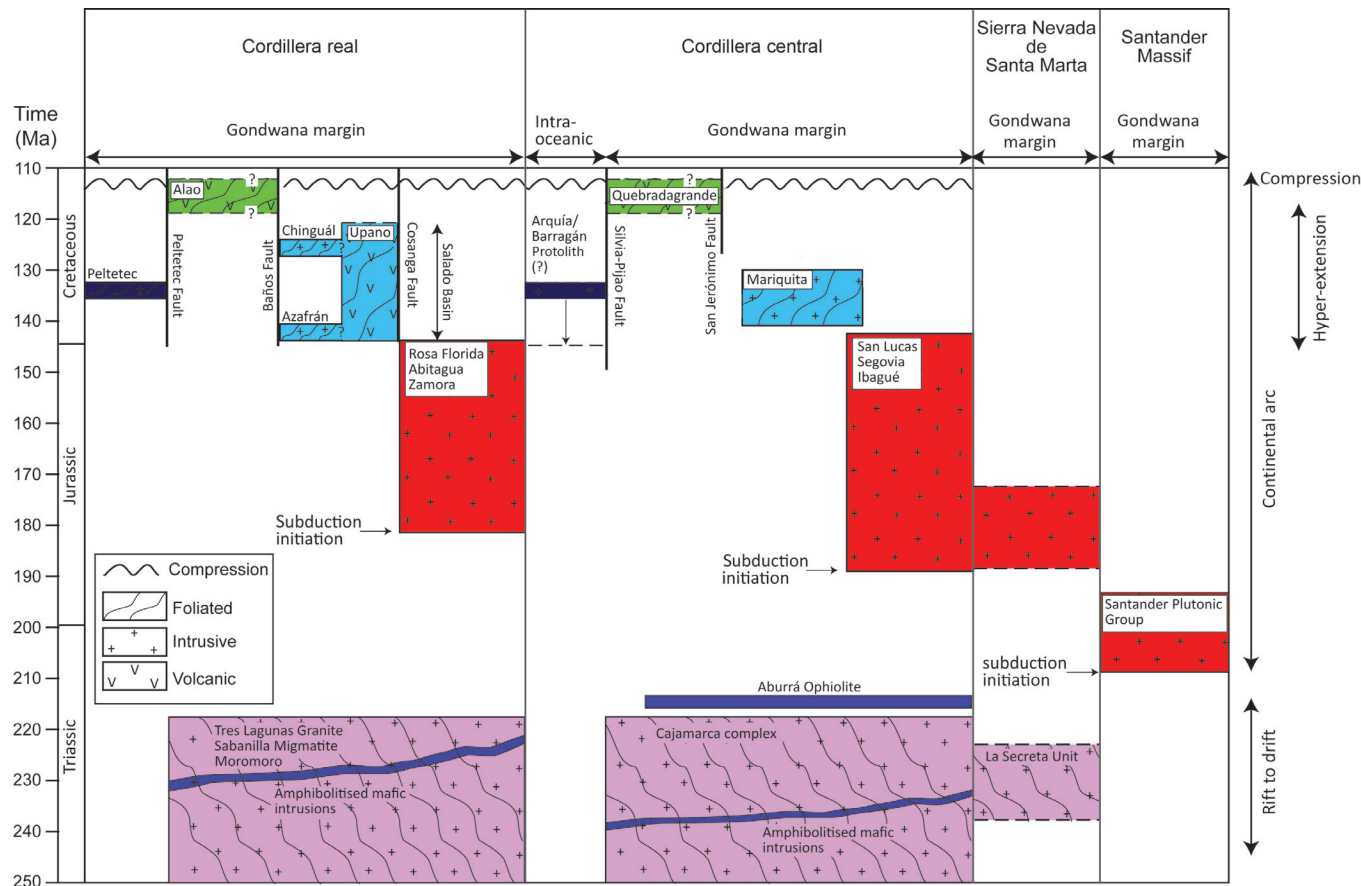
eclogites and blueschists of the Raspas unit (Litherland et al., 1994; Arculus et al., 1999; Bosch et al., 2002; John et al., 2010), which may be a tectonic equivalent of the Peltetec Unit (Spikings et al., 2015).

Within Colombia, metamorphosed igneous and sedimentary rocks of the Quebradagrande Complex are juxtaposed against the Triassic Cajamarca Unit in the Cordillera Central of Colombia via the San Jerónimo Fault, and thus they are located in a similar structural position as the Alao Arc in Ecuador (Figs. 1 and 2). The Quebradagrande Complex is exposed in highly deformed inliers along the entire length of the Cordillera Central. Lithologies are dominated by low-grade metamorphosed basalts, andesites, and pyroclastic rocks (e.g., Nivia et al., 2006; Villagomez et al., 2011; Rodriguez and Zapata, 2013; Jaramillo et al., 2017), and marine metasedimentary rocks that are covered by marine and terrestrial metasedimentary rocks of the Abejorral Fm., which hosts Hauterivian to lower Albian fossils (Gonzalez, 1980). The highly deformed nature of the Quebradagrande Complex led Maya and González (1995) to assign the term Quebradagrande Complex, which is used in this review. Fossil evidence suggests the sedimentary component was deposited during the Berriasian to Aptian (145–112 Ma using the timescale of Gradstein et al., 2004; see Nivia et al., 2006 and references therein). Other geochronological analyses include K/Ar dates (Toussaint et al., 1978), concordant U-Pb (zircon) dates of volcanic rocks (Villagomez et al., 2011; Cochrane et al., 2014a), and U-Pb dates of detrital zircons (Jaramillo et al., 2017). Geochemical analyses of the metavolcanic rocks are presented by Nivia et al. (2006), Villagomez et al. (2011), Rodriguez and Zapata (2013), Cochrane et al. (2014b), and Jaramillo et al. (2017). Tectonic interpretations vary from mid-ocean-ridge (e.g., Gonzalez, 1980; Bourgois et al., 1987), oceanic arc (Villagomez et al., 2011), continental arc (Cochrane et al., 2014b; Spikings et al., 2015; Jaramillo et al., 2017), and an intracratonic marginal basin (Nivia et al., 2006). Vasquez and Altenberger (2005) document small, lower Cretaceous intrusions within the Colombian Eastern Cordillera (Fig. 1), which they relate to rifting.

The Quebradagrande Complex is in contact with faulted slices of mafic igneous rocks that have been metamorphosed under medium-to-high-pressure and low-temperature conditions (Figs. 2 and 3). These are exposed in discontinuous, fault-bounded lenses along the strike of the Cordillera Central, and include the Arquía (e.g., Restrepo and Toussaint, 1976), Jambaló (Orrego et al., 1980; Bustamante et al., 2011), and Barragán (e.g., Bustamante et al., 2012) complexes, among others. These authors describe eclogite and blueschist facies metamorphic rocks (epidote glaucophane schists and chlorite-lawsonite schists), associated with amphibolites, metaultramafic rocks, serpentinites, and protocataclasites. Rocks exposed in the Jambaló region are faulted against the eastern margin of the Quebradagrande Complex (Bustamante, 2008), although the Arquía and Barragán sequences crop out to the west of the Quebradagrande Complex, across the Silvia-Pijao Fault, and their western margin is limited by the Cauca-Almaguer Fault (Fig. 2). Early radiometric dates of these rocks were K/Ar analyses (Feininger and Silberman, 1982),

#### FIG. 2, CONT'D

Geology of the Cordillera Central of Colombia and the Cordillera Real and Amotape Complex of Ecuador, showing the distribution of Early Cretaceous to Paleozoic rocks. A representative selection of zircon U-Pb concordia,  $^{40}\text{Ar}/^{39}\text{Ar}$  plateau and Lu-Hf isochron dates and their uncertainties ( $\pm 2\sigma$ ) obtained by various analytical methods (see Table 1 in the online version at <https://doi.org/10.1016/B978-0-12-816009-1.00009-5> for references) are shown. Some batholiths and plutons are labeled. Cities, I, Ibagué; L, Loja; M, Medellín; P, Pasto; Q, Quito. Faults: BF, Baños Fault; CAF, Cauca-Almaguer Fault; IF, Ibagué Fault; LF, Llanganates Fault; OPF, Otú-Pericos Fault; PF, Peltetec Fault. Map compiled from Litherland et al. (1994) and Gomez et al. (2007).

**FIG. 3**

Simplified stratigraphic scheme of magmatic rocks within the Santander Massif, Sierra Nevada de Santa Marta, Cordillera Central, and the Cordillera Real. Jurassic volcanic units are not shown. Sedimentary formations have been omitted. The general younging of the onset of latest Triassic-Jurassic intrusive magmatism is shown, along with a summary tectonic setting. See Table 1 in the online version at <https://doi.org/10.1016/B978-0-12-816009-1.00009-5> for references to geochronological data. The ages of the protolith of the amphibolites and blueschists of the Arquia and Barragán units are predicted assuming the subduction of young subducted Pacific lithosphere at the time of peak metamorphism (~129 Ma; see text).

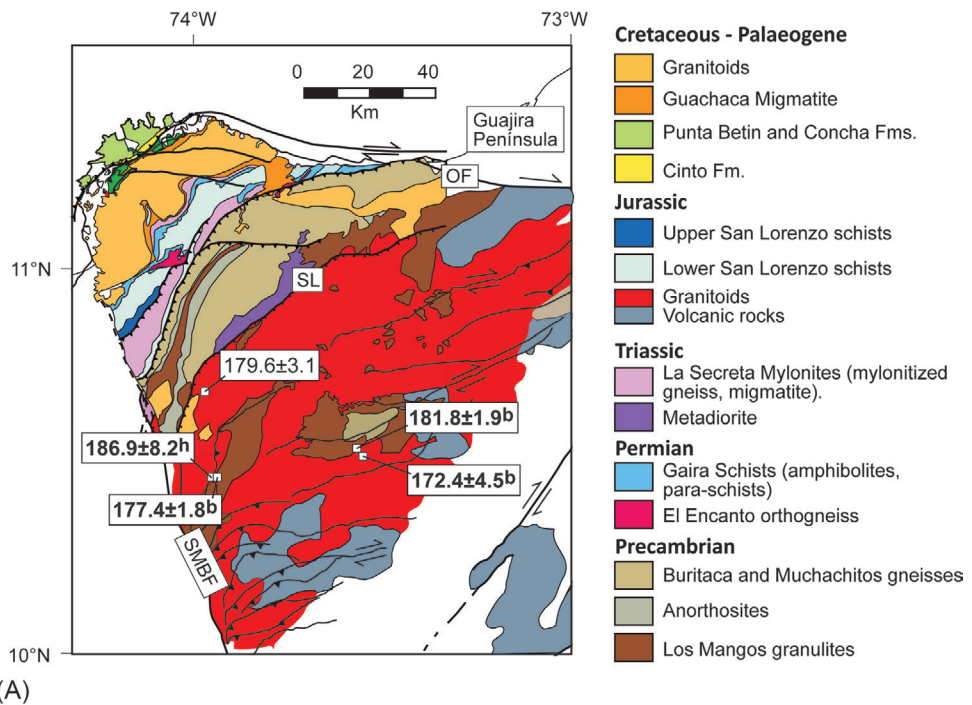
and numerous  $^{40}\text{Ar}/^{39}\text{Ar}$  dates have been reported (Villagomez et al., 2011; Bustamante et al., 2012). The Arquía and Barragán complexes occupy an equivalent tectonic position as the Peltetec and the Raspas complexes in the Cordillera Real and Amotape Terrane of Ecuador, respectively.

### 3 Geochronology

#### 3.1 Latest Triassic to earliest Cretaceous intrusions: Cordillera real, Cordillera central, Sierra Nevada de Santa Marta, and the Santander Massif

The most accurate estimates of the crystallization ages are provided by concordant U-Pb zircon dates (Fig. 2; Table 1 in the online version at <https://doi.org/10.1016/B978-0-12-816009-1.00009-5>), which range between 194 and 209 Ma in the Santander Massif (Mantilla Figueroa et al., 2013; Van der Lelij et al., 2016), 130–193 Ma in the Cordillera Central (Bustamante et al., 2010, 2016; Villagomez et al., 2011; Cochrane et al., 2014b; Spikings et al., 2015; Rodriguez et al., 2018), and 141–182 Ma in the Cordillera Real (Chiaradia et al., 2009; Cochrane et al., 2014b; Spikings et al., 2015). Acidic intrusions dominate exposure of the Sierra Nevada Block of the Sierra Nevada de Santa Marta (northern Colombia; Fig. 4A), and the few radiometric dates that exist include a Jurassic U-Pb (zircon) age of  $179.6 \pm 13.1$  Ma (Colmenares, 2007), and new (this study) Jurassic  $^{40}\text{Ar}/^{39}\text{Ar}$  plateau dates spanning between 172 and 187 Ma (hornblende and biotite; this study; Fig. 4; Table 2 in the online version at <https://doi.org/10.1016/B978-0-12-816009-1.00009-5>), although these  $^{40}\text{Ar}/^{39}\text{Ar}$  dates likely represent minimum crystallization ages. Leal-Mejia et al. (2011) report a range of zircon U-Pb dates from the Santander Massif and Cordillera Central (210–149 Ma), although they do not present their data, and thus they cannot be evaluated.

A comparison of zircon U-Pb age and latitude (Fig. 5) suggests that the timing of the onset of magmatism may become younger from northern Colombia to southern Ecuador. The Jurassic intrusions of the Sierra Nevada de Santa Marta break this trend, which may reflect post-Jurassic displacement of these rocks from southern latitudes (Bayona et al., 2010). These data also suggest that Jurassic arc magmatism did not initiate south of approximately 2.5°S until ~182 Ma, although this trend may be an artifact of sampling density. A second chronological trend is seen when the crystallization ages are compared with their distance from the equivalent Silvia-Pijao (Colombia) and Peltetec (Ecuador) Faults (Fig. 6B), indicating that Jurassic magmatism becomes younger as it approaches the approximate location of the contemporaneous plate margin. Assuming insignificant strike-slip displacement, this implies that Jurassic magmatism initiated far from the trench at ~209 Ma, and these rocks are currently exposed within the Santander Massif (209–194 Ma; Fig. 2; Mantilla Figueroa et al., 2013; Van der Lelij et al., 2016) and in the region of Mocoa in the far southern Cordillera Central (Leal-Mejia et al., 2011). Magmatism migrated westwards at ~195 Ma and stabilized within the region that is now exposed within the Cordilleras Central and Real, and the flanks of the Upper Magdalena Valley, throughout the Jurassic. The older magmatic belt (>189 Ma) is not exposed, or did not form in Ecuador. The youngest Jurassic intrusions of the foliated Azafrán Batholith (141–144 Ma; Table 1 in the online version at <https://doi.org/10.1016/B978-0-12-816009-1.00009-5>) occur to the west of the mainly unfoliated intrusions (Fig. 6) of the Rosa Florida, Abitagua and Zamora batholiths (145–189 Ma) in Ecuador. The Mariquita Stock (130–143 Ma; Table 1 in the online version at <https://doi.org/10.1016/B978-0-12-816009-1.00009-5>) in Colombia temporally overlaps with the Azafrán Batholith. The range in dates of the unfoliated Jurassic intrusions closely overlaps with the age of Jurassic arc magmatism recorded in southern Peru (Fig. 5), Patagonia and northern Chile (195–147 Ma; zircon U-Pb and K/Ar dates; Scheuber and González, 1999; Rapela et al., 2005; Castro et al., 2011).



(A)

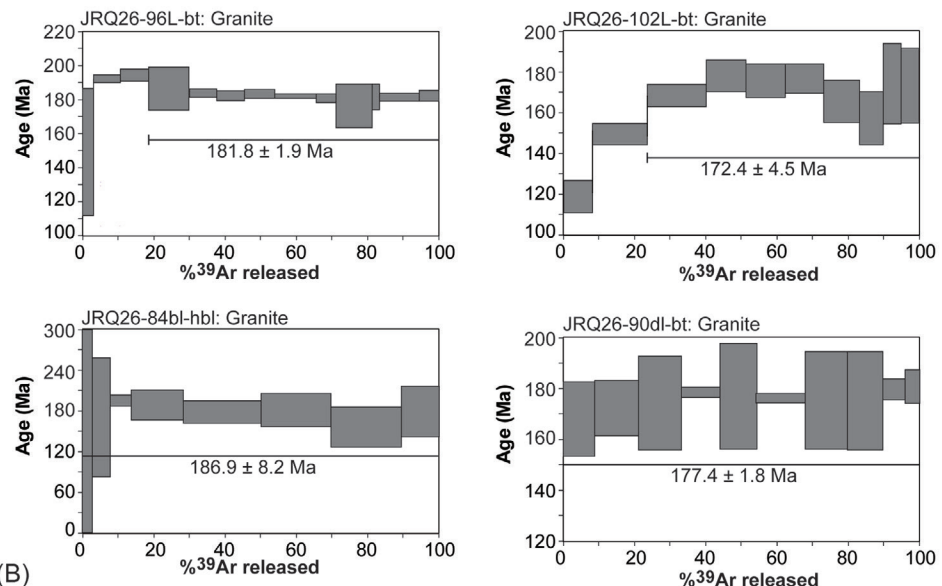
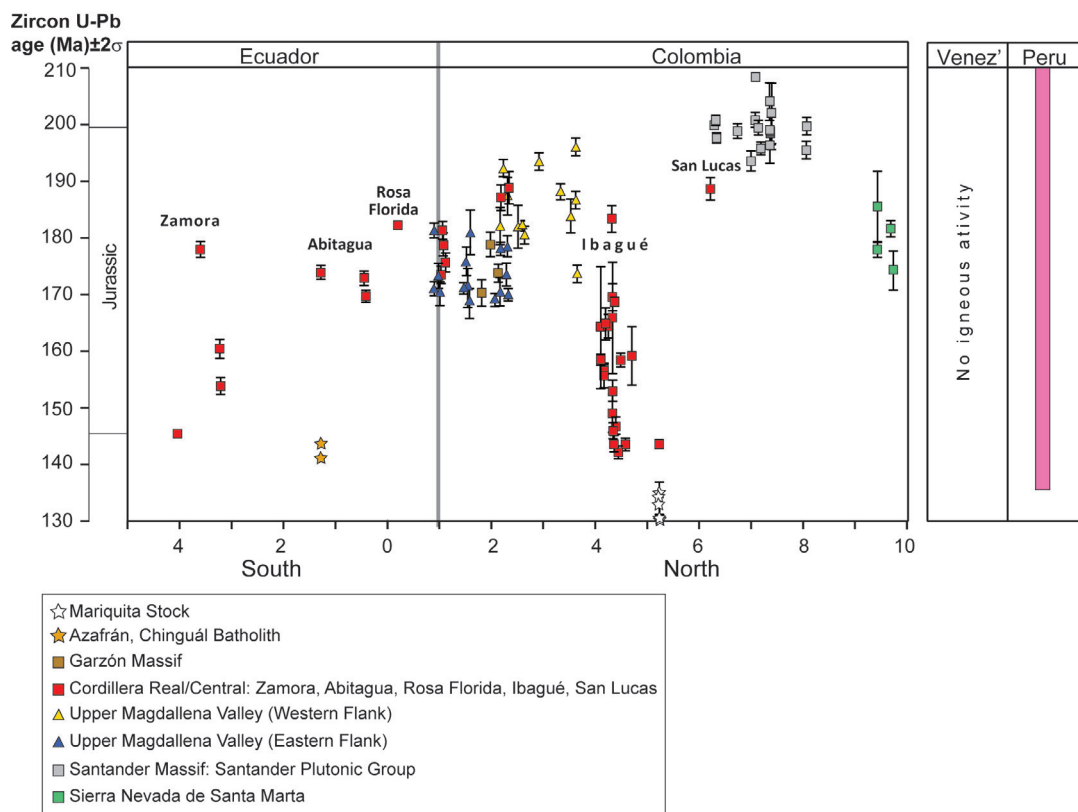


FIG. 4

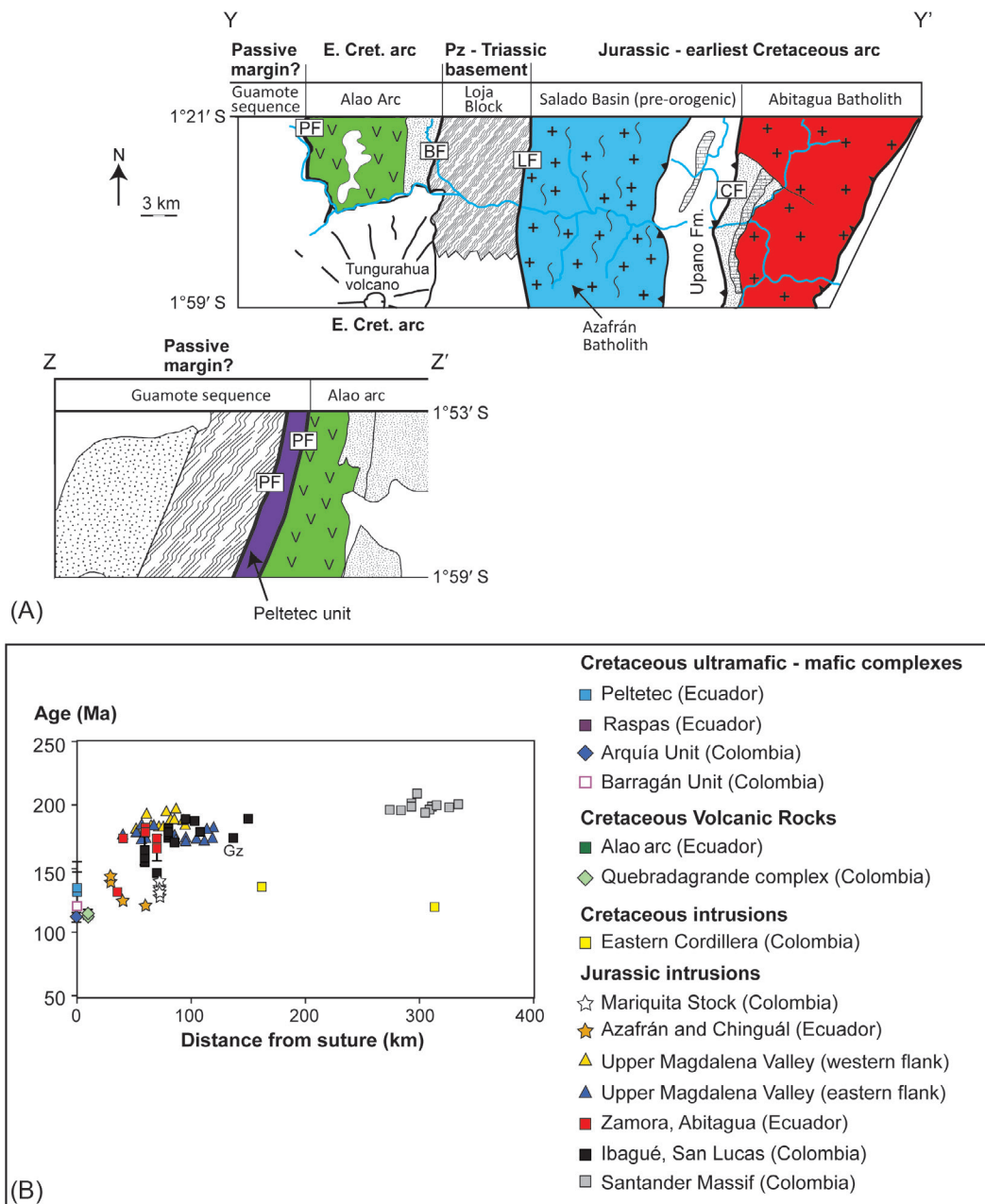
(A) Geological map of the Sierra Nevada de Santa Marta after Tschanz et al. (1974), Ingeominas (2007a,b), and Piraquive (2017), showing the main structural belts.  $^{40}\text{Ar}/^{39}\text{Ar}$  plateau dates (this study; Table 2 in the online version at <https://doi.org/10.1016/B978-0-12-816009-1.00009-5>) and a single zircon U-Pb concordia date (Colmenares, 2007) of Jurassic intrusions (Table 1 in the online version at <https://doi.org/10.1016/B978-0-12-816009-1.00009-5>) are shown. h, hornblende; b, biotite. OF, Oca Fault; SL, Sevilla Lineament. Legend for geochronological data is the same as that shown in Fig. 2. (B)  $^{40}\text{Ar}/^{39}\text{Ar}$  age spectra (IR-CO<sub>2</sub> laser step-heating) obtained in the current study for the granitoids shown in (A). Data were acquired using the methodology described in Villagomez and Spikings (2013), including the parameters described in Table 2 in the online version at <https://doi.org/10.1016/B978-0-12-816009-1.00009-5>.

**FIG. 5**

A comparison of latest Triassic-Jurassic concordant zircon U-Pb dates with latitude along the Cordillera Real, Cordillera Central, margins of the Upper Magdalena Valley, and the Santander and Garzón massifs of Colombia. The ranges of concordant zircon U-Pb dates obtained from granitoid intrusions and volcano-sedimentary rocks from the Eastern Cordillera (Miskovic et al., 2009) and Arequipa Terrane of Peru (Boekhout et al., 2012; Demouy et al., 2012) are shown for comparison. Data and citations are presented in Table 1 in the online version at <https://doi.org/10.1016/B978-0-12-816009-1.00009-5>.

### 3.2 Early Cretaceous magmatic and sedimentary rocks: Cordillera Real and Cordillera Central

Within the Cordillera Real of Ecuador, a meta-andesite of the Upano Unit yields a zircon U-Pb crystallization age of  $121.0 \pm 0.8$  Ma (Cochrane et al., 2014b; Table 1 in the online version at <https://doi.org/10.1016/B978-0-12-816009-1.00009-5>).  $^{238}\text{U}$ - $^{206}\text{Pb}$  dates from the rims and cores of detrital zircons extracted from a quartzite of the Upano Fm. (Cochrane et al., 2014b) reveal a large spread in ages from rims and cores, and the youngest age of  $143.3 \pm 9.9$  Ma constrains its maximum stratigraphic age. The Upano Unit is considered to have been deposited in the pre-orogenic Salado Basin (Figs. 3 and 6), although the stratigraphic relationship between the andesite and the quartzite is uncertain due to

**FIG. 6**

(A) Strip maps across the central Cordillera Real of Ecuador, after Litherland et al. (1994). Sections (Y-Y' and Z-Z') are labeled in Fig. 2. (B) Relationship between zircon U-Pb concordia age and distance from the Peltetec-Silvia-Pijao Fault, which is considered to represent the Jurassic-Early Cretaceous paleo-margin. Citations for the age data are provided in Table 1 in the online version at <https://doi.org/10.1016/B978-0-12-816009-1.00009-5>. Gz, Garzón Massif.

complicated structural relationships. The Chinguál and Azafrán batholiths yield concordant U-Pb zircon ages of  $125.3 \pm 0.9$  Ma and 141–144 Ma, respectively (Cochrane et al., 2014b; Figs. 2 and 3; Table 1 in the online version at <https://doi.org/10.1016/B978-0-12-816009-1.00009-5>). Pratt et al. (2005) suggest the contact between the Azafrán Batholith and the Upano Unit is unconformable, while Litherland et al. (1994) claim it is faulted (Fig. 6). U-Pb age peaks of detrital zircons in the Upano Unit occur at 500–600 Ma, 900–1200 Ma, 1500 Ma, and the oldest is ~2 Ga (Spikings et al., 2015). The maximum stratigraphic age is consistent with pollen assemblages that have a poorly resolved Early Jurassic-Cretaceous age (Riding, 1989). Granodiorites of the Mariquita Stock (Central Cordillera, Colombia) yield zircon U-Pb dates that range between 130 and 143 Ma (Bustamante et al., 2016; Figs. 2 and 3; Table 1 in the online version at <https://doi.org/10.1016/B978-0-12-816009-1.00009-5>), which are similar to those obtained from the Chinguál and Azafrán batholiths in Ecuador. Bustamante et al. (2016) report that the Mariquita stock intrudes the Cajamarca Complex, which was deposited in the Triassic (Villagomez et al., 2011; Cochrane et al., 2014a; Spikings et al., 2015).

No zircon U-Pb dates have been obtained from the metavolcanic rocks of the Alao Arc in Ecuador, located west of the Triassic anatectites and the Baños Fault (Fig. 2). Litherland et al. (1994) report imprecise K/Ar (hornblende) dates of  $115 \pm 12$  Ma and  $142 \pm 36$  Ma, and pollen assemblages suggest the volcanoclastic sedimentary rocks are Middle Jurassic (Riding, 1989). If the pollen occurrence is accurately calibrated against absolute time, then the K/Ar hornblende dates are partially reset.  $^{238}\text{U}$ - $^{206}\text{Pb}$  dates from the rims and cores of detrital zircons extracted from a quartzite of the Alao Arc (Cochrane et al., 2014b) yield a minimum age of  $163.7 \pm 1.6$  Ma (Fig. 2; Table 1 in the online version at <https://doi.org/10.1016/B978-0-12-816009-1.00009-5>), constraining its maximum stratigraphic age. Similar detrital age populations are found compared to the detrital dates from the Upano Unit, suggesting they were supplied by the same source regions. Furthermore, Early Ordovician acritarchs suggest they have been reworked into the Alao arc sequence (Litherland et al., 1994), corroborating the detrital zircon U-Pb age spectrum (Spikings et al., 2015). We conclude that no reliable age dates exist for the Alao arc, although it is Middle Jurassic, or younger. Within Colombia, Villagomez et al. (2011) and Cochrane et al. (2014b) report concordant zircon U-Pb dates of magmatic rocks of the Quebradagrande Fm. of  $114.3 \pm 3.8$  Ma (tuff) and  $112.9 \pm 0.8$  Ma (diorite; Figs. 2 and 3; Table 1 in the online version at <https://doi.org/10.1016/B978-0-12-816009-1.00009-5>). Toussaint and Restrepo (1994) report a K/Ar (whole rock basalt) date of  $105 \pm 0.8$  Ma, although it is likely to be at least partially reset. The U-Pb dates are consistent with Berriasian to Aptian (145–112 Ma; Nivia et al., 2006 and references therein) fossil dates, and a maximum stratigraphic age of ~149 Ma obtained from detrital zircons (Cochrane et al., 2014b). Vasquez et al. (2010) report hornblende  $^{40}\text{Ar}$ / $^{39}\text{Ar}$  (plateau) dates of  $120.5 \pm 0.6$  Ma (tuff) and  $136.0 \pm 0.4$  Ma (diorite) from small gabbroic intrusions located in the Eastern Cordillera of Colombia (Figs. 1 and 11; Table 1 in the online version at <https://doi.org/10.1016/B978-0-12-816009-1.00009-5>). Jaramillo et al. (2017) report a zircon a U-Pb date of  $93.4 \pm 0.5$  Ma from a diorite that intrudes the Quebradagrande Complex. They consider the diorite to form part of the Quebradagrande Complex, although no clear justification is provided.

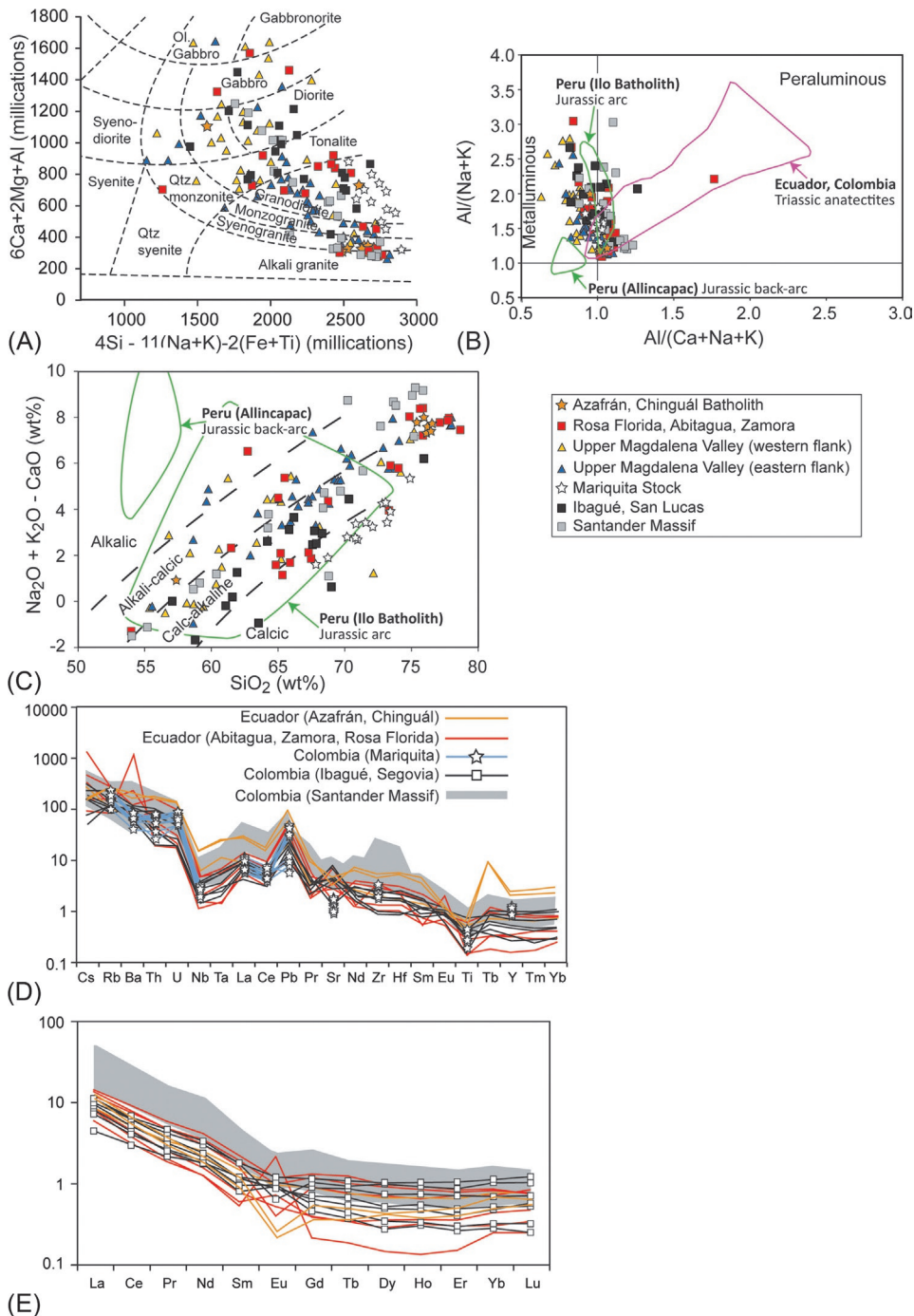
Dating the crystallization ages of the mafic and ultramafic protoliths of the MP-HP/LT rocks of the Arquía, Barragán, Jambaló, Peltetec, and Raspas complexes (Figs. 1 and 2) is problematic due to metamorphic overprinting, and the lack of high-U, low-(common)Pb minerals, and no U-Pb dates have been published. Bustamante et al. (2012) present a weighted mean  $^{40}\text{Ar}$ / $^{39}\text{Ar}$  date from three plateau white mica dates of  $120.7 \pm 0.6$  Ma (Fig. 2; Table 1 in the online version at <https://doi.org/10.1016/B978-0-12-816009-1.00009-5>) from a single muscovite schist of the Barragán Complex, which they suggest records

retrogression during exhumation. This Early Cretaceous date is similar to a plateau hornblende  $^{40}\text{Ar}/^{39}\text{Ar}$  date of  $112.0 \pm 3.7$  Ma (Villagomez et al., 2011) obtained from the Arquía Complex, which has also been interpreted as the time of retrogression. The only other interpretable dates from Colombia are plateau  $^{40}\text{Ar}/^{39}\text{Ar}$  white mica (paragonite and phengite) dates from blueschists of the Jambaló Complex, which range between 68 and 62 Ma (Bustamante et al., 2011), which were interpreted to record the mylonitic event that was responsible for exhuming the rocks. Numerous dates have been obtained from eclogites and blueschists of the Raspas Complex in the Amotape Complex (Ecuador). Phengite K/Ar (Feininger and Bristow, 1980) and  $^{40}\text{Ar}/^{39}\text{Ar}$  dates (Gabriele, 2002) of  $132 \pm 5$  Ma and 123–129 Ma (Fig. 2) were interpreted to record cooling during retrogression of the eclogites. However, these dates must be interpreted with caution, given the propensity for phengite in high-pressure rocks to incorporate excess  $^{40}\text{Ar}$ . John et al. (2010) report Lu-Hf isochron (garnet, whole rock, amphibole, pyroxene) ages of  $126.4 \pm 4.0$  and  $129.9 \pm 5.6$  Ma, while the older estimate is considered to be more accurate, given its MSWD of 2.0 (Table 1 in the online version at <https://doi.org/10.1016/B978-0-12-816009-1.00009-5>). These dates are interpreted to record garnet growth (John et al., 2010), and overlap with the phengite  $^{40}\text{Ar}/^{39}\text{Ar}$  dates of Gabriele (2002). Mafic and ultramafic assemblages of the Peltetec sequence have only experienced greenschist grade metamorphism, and yield  $^{40}\text{Ar}/^{39}\text{Ar}$  plateau dates of  $134.7 \pm 0.9$  Ma and  $134 \pm 13$  Ma (Table 1 in the online version at <https://doi.org/10.1016/B978-0-12-816009-1.00009-5>), which are interpreted as the minimum crystallization ages of the basaltic protolith (Spikings et al., 2015; Fig. 3).

## 4 Geochemistry

### 4.1 Latest Triassic-earliest Cretaceous granitoids

Latest Triassic to Earliest Cretaceous (209–130 Ma) magmatic rocks in the Cordillera Real, Cordillera Central, and the Santander Massif are dominated by granitic to dioritic intrusions, with minor gabbros (Fig. 7A). The rocks are mildly peraluminous to metaluminous (Fig. 7B), and plot in the calc-alkaline to alkali-calcic field of Frost et al. (2001) (Fig. 7C), and in the high-K calc-alkaline and calc-alkaline fields when comparing immobile elements (Fig. 8A). Negative Nb, Ta, and Ti anomalies, combined with enriched LILE (Light Ion Lithophile Elements) relative to HFSE (High Field Strength Elements), and LREE (Light Rare Earth Elements) relative to HREE (Heavy Rare Earth Elements), suggest these rocks formed in a subduction-related setting and they are interpreted as continental arc intrusions (Fig. 7D and E). Granitoids from the Santander Massif, which were probably located furthest from the plate margin, are slightly more enriched in LILE and are more peraluminous than the younger granitoids, which intruded closer to the paleotrench. The magmas within the Santander Massif may have assimilated more continental crust, perhaps because the crust was thicker. Finally, the trace and major elements reveal no along-strike geochemical differences in the magmas that formed within the Ecuador and Colombia (Fig. 7).  $\epsilon\text{Nd}_i$  (whole rock) values for the latest Triassic-Earliest Cretaceous granitoids range between -7.2 and 5.3, and the oldest intrusions, which are exposed in the Santander Massif, host distinctly less radiogenic Nd isotopic compositions than younger intrusions located further west (Fig. 8B).  $\epsilon\text{Nd}_i$  (whole rock) values from the unfoliated intrusions of the cordilleras Real and Central (red and black symbols in Fig. 8B) define no particular trend.  $\epsilon\text{Hf}_i$  (zircon) has a large range of -6 to 9.25 (Fig. 8C), and a well-defined trend indicates that the isotopic composition becomes more radiogenic as the rocks become younger, although a large range in  $\epsilon\text{Hf}_i$  (zircon) can be found in the unfoliated intrusions of the cordilleras Real and Central, at any given time. The youngest, foliated intrusions in Ecuador (Chinguál and Azafrán) are located to the west

**FIG. 7**

See figure caption on opposite page.

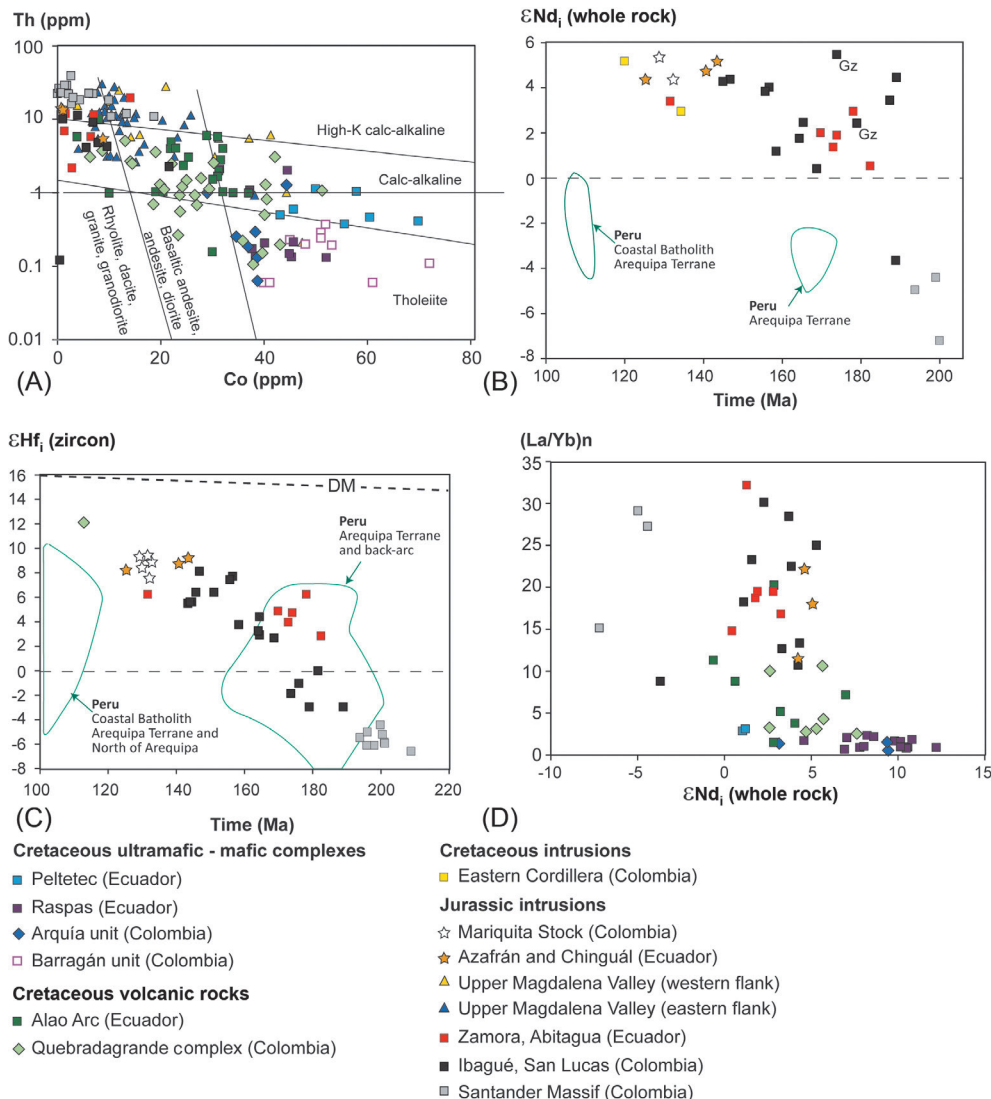
of the older granitoids and yield the most juvenile isotopic compositions. The same relationship is found in the Cordillera Central, where Early Cretaceous (130–143 Ma; Bustamante et al., 2016) granodiorites of the Mariquita Stock (Fig. 7A), yield relatively radiogenic  $\epsilon_{\text{Nd}_i}$  (whole rock) and  $\epsilon_{\text{Hf}_i}$  (zircon) values compared to the Jurassic Ibagué Batholith. These trends suggest that the latest Triassic-earliest Cretaceous intrusions become more juvenile as the intrusions migrate toward the paleo-plate margin. The arc intrusions were intruding through continental crust that was becoming thinner between ~194 and ~189 Ma, and during the latest Jurassic-earliest Cretaceous, starting at ~143 Ma (Azafrán and Chinguál intrusions). This could be interpreted as extension along the plate margin, and migration of the arc axis toward the trench.

## 4.2 Early Cretaceous igneous rocks

Dacites, andesites, basalts, and gabbros of the Quebradagrande (Colombia) and Alao (Ecuador) sequences are metaluminous and span a larger range in Aluminum Saturation Index than the Early Triassic-earliest Cretaceous intrusions (Fig. 9A). Tectonic discrimination diagrams suggest that these rocks formed in a variety of tectonic environments, spanning from calk-alkaline arc to island arc tholeiite, ocean plateau tholeiite, and MORB compositions (Fig. 9B and C). These observations corroborate (i) the N-MORB normalized REE plot (Fig. 9E), which reveals both N-MORB-like compositions, and rocks that are enriched in LREE, which is more characteristic of subduction-related rocks, and (ii) the N-MORB normalized trace element plot (Fig. 9D), which shows that some samples have characteristic negative Nb, Ta, and Ti anomalies, while these are missing in the rocks that yield almost flat REE patterns. These rock sequences are exposed within faulted blocks, and distinguishing between rock sequences that form the Quebradagrande Complex and the juxtaposing Arquía Complex is difficult in the field. Therefore, we suggest that some of the basalts that yield N-MORB signatures may be a structurally separated component of the Arquía or Peltetec complexes, which yield MORB and E-MORB signatures (see later), and are now intercalated within arc rocks of the Quebradagrande and Alao sequences.  $\epsilon_{\text{Nd}_i}$  (whole rock; Fig. 8D) from the volcanic rocks of the Quebradagrande and Alao sequences ranges between –0.64 and 7.63 (Table 1 in the online version at <https://doi.org/10.1016/B978-0-12-816009-1.00009-5>), and there is a general reduction in  $(\text{La}/\text{Yb})_n$  as  $\epsilon_{\text{Nd}_i}$  (whole rock) becomes more radiogenic (Fig. 8D). The least radiogenic basalts within these volcanic sequences are more juvenile than the most radiogenic Nd isotopic compositions obtained from the Jurassic granitoids. Similarly, the single  $\epsilon_{\text{Hf}_i}$  (zircon) measurement from the Quebradagrande Complex (Cochrane et al., 2014b) is more radiogenic than the same measurements from the Jurassic granitoids (Fig. 8C).

### FIG. 7, CONT'D

Geochemical data from latest Triassic (209 Ma)-earliest Cretaceous (130 Ma) intrusions from the Cordillera Real, Cordillera Central, margins of the Upper Magdalena Valley (major oxides only) and the Santander Massif (Litherland et al., 1994; Romeuf et al., 1995; Bustamante et al., 2010; Cochrane et al., 2014b; Van der Leij et al., 2016; Rodriguez et al., 2018). Lithological discriminatory fields shown in (A) are from Batchelor and Bowden (1985), (B) are from Maniar and Piccoli (1989), and (C) are from Peacock (1931). Fields are shown for Jurassic intrusions within the Arequipa Terrane (Boekhout et al., 2012; Demouy et al., 2012) and the Alliancapac Complex (Miskovic et al., 2009) of Peru. Multielement plots (D and E) are normalized to N-MORB (Sun and McDonough, 1989) and do not include trace element data for intrusions that crop out along the flanks of the Upper Magdalena Valley.

**FIG. 8**

Geochemical and isotopic data from latest Triassic (209 Ma)-earliest Cretaceous (130 Ma) intrusions, and Early Cretaceous volcanic rocks, and M-HP/LT mafic and ultramafic rocks from the Cordillera Real, Cordillera Central, Santander Massif, margins of the Upper Magdalena Valley and the Eastern Cordillera of Colombia. Data are from Litherland et al. (1994), Romeuf et al. (1995), Bustamante et al. (2010), Cochrane et al. (2014b), Bustamante et al. (2016), Van der Lelij et al. (2016), and Rodriguez et al. (2018). Fields for the Coastal Batholith of Peru are from data in De Haller et al. (2006), Demouy et al. (2012), Boekhout et al. (2013), and unpublished data from U. Schaltegger (University of Geneva). Fields for the Arequipa Terrane and Jurassic back-arc of Peru are from data in Miskovic et al. (2009), Demouy et al. (2012), and Boekhout et al. (2013).

Blueschists and amphibolites of the Barragán and Arquía complexes yield flat REE (N-MORB normalized) multielement plots ( $(\text{La/Yb})_{\text{n}}$  0.74–4.68), and their trace element abundances lack strongly negative Nb, Ta, and Ti anomalies (Fig. 9F and G), contrasting with arc-related andesites and basalts of the Quebradagrande Unit, which is usually faulted against their eastern margin. These features are consistent with a tholeiitic fractionation trend (Fig. 8A), and juvenile  $\epsilon\text{Nd}_{\text{i}}$  (whole rock) values of 3.2–9.6

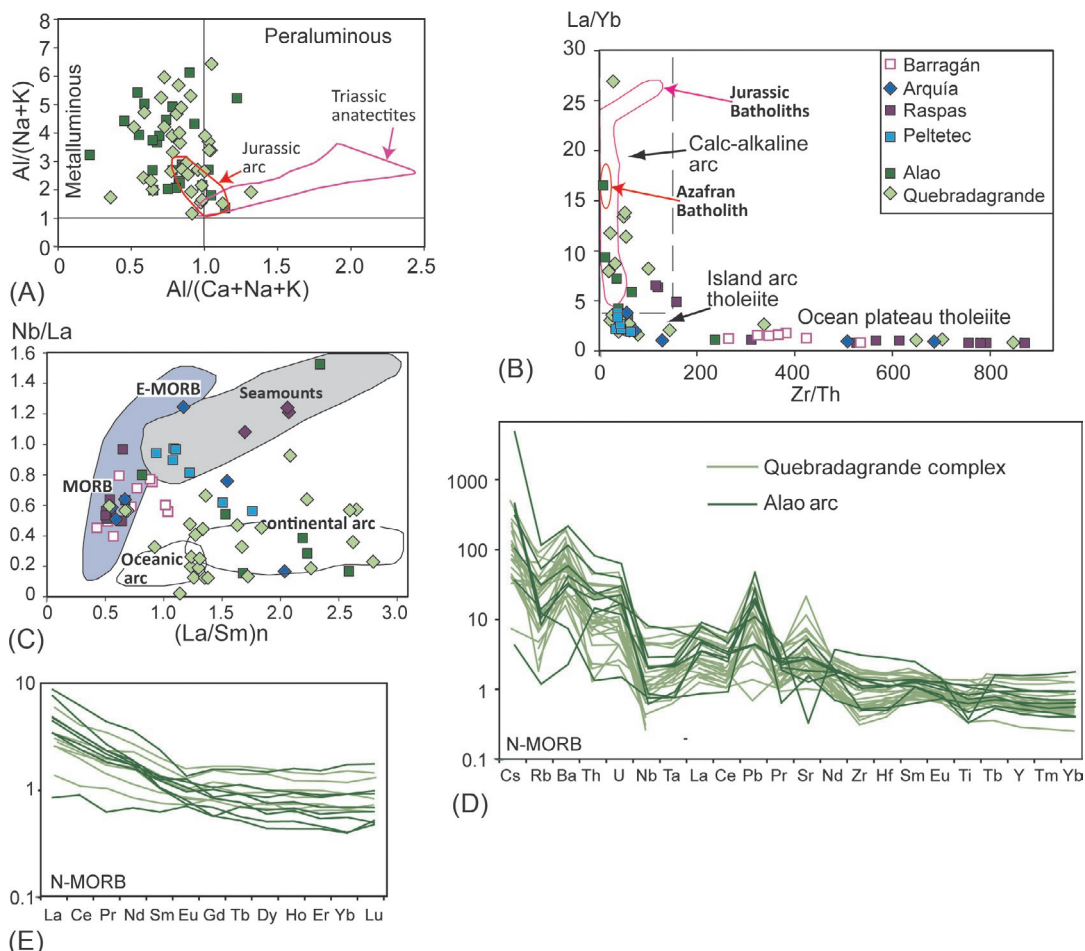


**FIG. 9**

Geochemical data from Early Cretaceous volcanic rocks (Litherland et al., 1994; Villagomez et al., 2011; Nivia et al., 2006; Cochrane et al., 2014b; Rodriguez and Zapata, 2013) and M-HP/LT mafic and ultramafic rocks (Litherland et al., 1994; Arculus et al., 1999; Bosch et al., 2002; John et al., 2010; Villagomez et al., 2011; Bustamante et al., 2012; Cochrane et al., 2014b) of the Amotape Complex and Cordillera Real of Ecuador, and the Cordillera Central of Colombia. La/Yb and Zr/Th tectonic discrimination fields are from Jolly et al. (2001), and the Th-Co classification of igneous rocks and tectonic environments is based on Hastie et al. (2007). Multielement plots are normalized to N-MORB (Sun and McDonough, 1989).

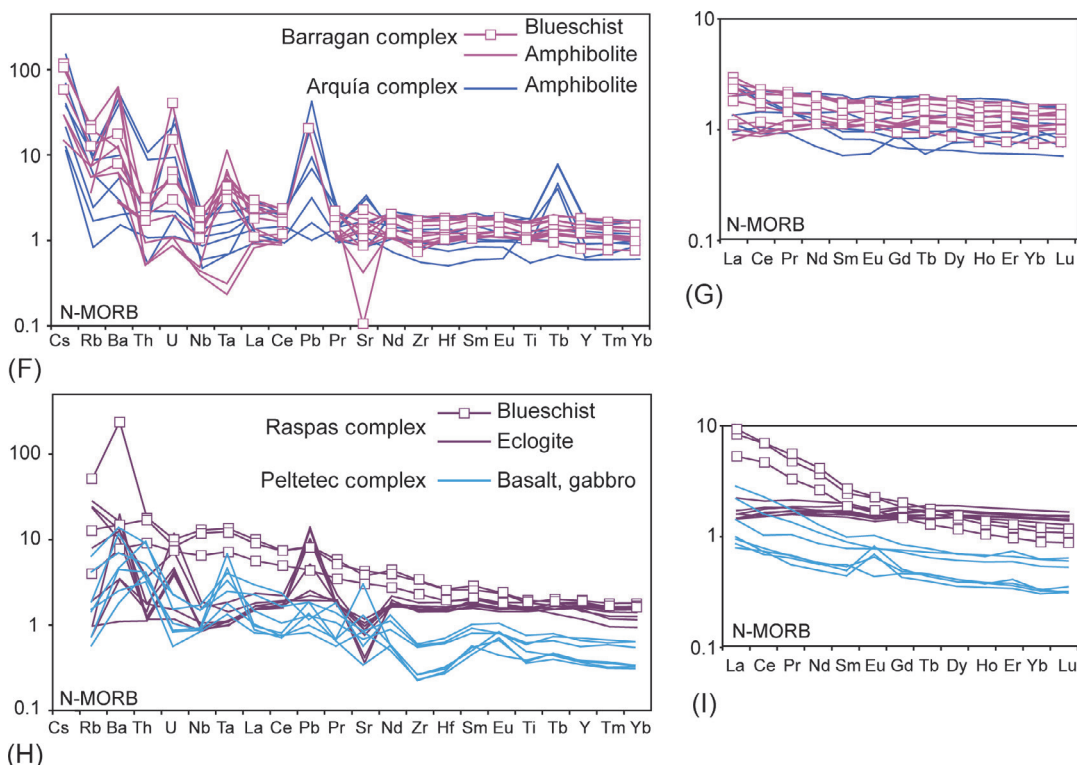


FIG. 9, CONT'D

(Arquía Complex only; Fig. 8D), which are more radiogenic than the Early Cretaceous volcanic rocks of the Quebradagrande unit. The MP-HP/LT metamorphosed rocks plot in the MORB to E-MORB field when comparing Nb/La with (La/Sm)n (Fig. 9C), and island arc to ocean-plateau tholeiite field when comparing La/Yb and Zr/Th (Fig. 9B). Bustamante et al. (2012) suggest that the protoliths to the blueschists and amphibolites of the Barragán Complex were normal midocean ridge basalts. Similarly, Villagomez et al. (2011) suggest the protolith to the amphibolites of the Arquía Complex may have formed at a midocean ridge.

Metamorphosed ultramafic-mafic rocks of the Raspas and Peltetec complexes in Ecuador are geochemically similar to the Barragán and Arquía units in Colombia. Eclogites of the Raspas Complex yield flat REE profiles when normalized against N-MORB ( $(\text{La/Yb})_n$  0.69–2.20; Arculus et al., 1999; Bosch et al., 2002; John et al., 2010), and their LILE contents are not significantly enriched relative to the HFSE, while negative Nb, Ta, and Ti anomalies are missing (Fig. 9H and I). The eclogites plot in the N-MORB field when comparing Nb/La with (La/Sm)n (Fig. 9C), and in the ocean plateau tholeiite field when comparing La/Yb and Zr/Th (Fig. 9B).  $\varepsilon_{\text{Nd}_i}$  (whole rock) values for the eclogites are juvenile, and range between 6.9 and 10.8 (Bosch et al., 2002; Fig. 8D), corroborating their depleted chemical compositions. In contrast, the blueschists from the Raspas Complex have enriched LILE relative to their HFSE, and elevated LREE relative to their HREE ( $(\text{La/Yb})_n$  6.0–7.9; John et al., 2010; Fig. 9H and I). The blueschists plot in the seamount field when comparing Nb/La with (La/Sm)n (Fig. 9C),

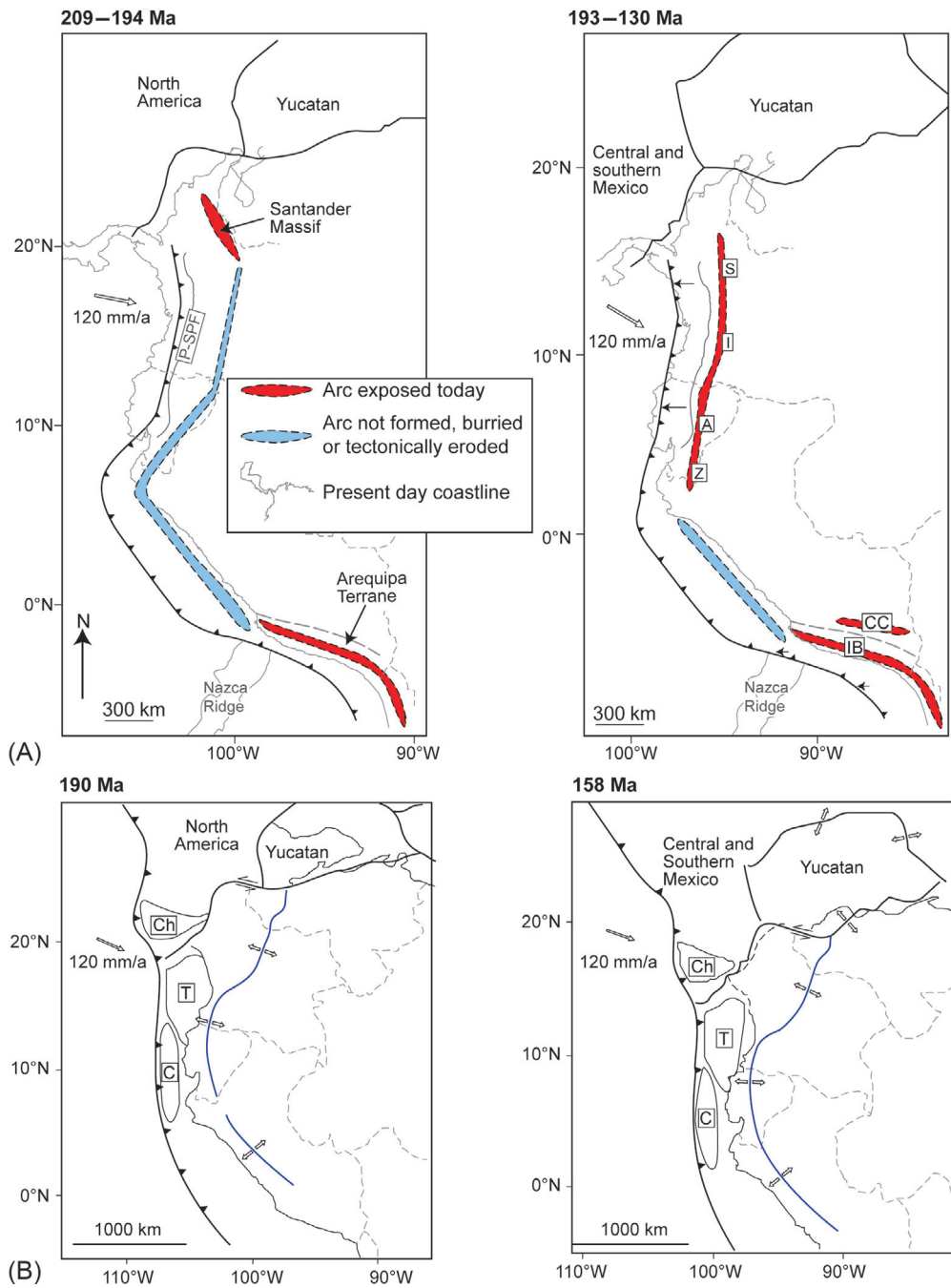
and in island arc tholeiite field when comparing La/Yb and Zr/Th, although they lack Nb, Ta, and Ti anomalies when normalized against N-MORB. [John et al. \(2010\)](#) ([Fig. 9H](#)) interpret the eclogites as subducted oceanic lithosphere that was typical of N-MORB, whereas the protoliths to the blueschists were considered to be seamounts. [Bosch et al. \(2002\)](#) suggest that the mafic and ultramafic rocks metamorphosed under high-pressure conditions and originally formed part of an oceanic plateau, while [Arculus et al. \(1999\)](#) report that the protoliths originated as both N-MORB, and within an oceanic plateau, and equilibrated with peak conditions at 1.3–2.0 GPa and  $\leq 600^{\circ}\text{C}$ . Finally, altered gabbros and basalts of the Peltetec unit, which is exposed within the Peltetec Fault Zone (Ecuador; [Fig. 6](#)), have received less attention, and the only available geochemical data are from [Litherland et al. \(1994\)](#), and new data that are published in this review (supplementary material). These rocks are generally depleted compared to the other mafic rocks (45–50 wt% SiO<sub>2</sub>; [Cochrane et al., 2014b](#); [Fig. 9H](#)) that lie in a similar structural position in Ecuador and Colombia, with lower trace element and REE abundances, and they yield slightly enriched LREE relative to HREE ((La/Yb)n 2.3–4.6; [Fig. 9I](#)), while there is a general absence of distinctive Nb, Ta, and Ti anomalies when normalized against N-MORB. The trace element abundances plot close to unity when normalized against N-MORB, and it is very likely that the LILE trends have been disturbed by alteration. The gabbros and basalts plot within the calc-alkaline to tholeiitic field when comparing immobile elements ([Fig. 8A](#)), and a majority of the rocks plot within the MORB-seamount field when comparing Nb/La against (La/Sm)n ([Fig. 9C](#)).  $\epsilon\text{Nd}_i$  (whole rock) values for the Peltetec unit range between 1.1 and 1.2 ([Spikings et al., 2015](#); [Fig. 8D](#)), and they are less radiogenic than those obtained from other mafic rocks (45–50 wt% SiO<sub>2</sub>; [Cochrane et al., 2014b](#)) that lie in a similar structural position in Ecuador and Colombia. We interpret these data to suggest the protolith to these greenschist facies formed either within an ocean plateau, or perhaps within a back-arc basin setting, as transitional crust.

## 5 Discussion

### 5.1 The tectonic setting during the latest Triassic-Jurassic (209–130 Ma)

A combination of field studies, concordant zircon U-Pb dates, geochemistry and isotopic data clearly shows that an I-type, metaluminous, high-K to calc-alkaline continental arc started to form within northwestern South America at ~209 Ma, due to subduction of Pacific oceanic lithosphere beneath western South America. This time period marks the formation of a new subduction zone inboard of the Central and North American terranes that were the Permo-Triassic conjugate margin to northern South America within Pangaea. Arc magmatism during 194–209 Ma was focused within the rocks of the Santander Massif, currently located 280–350 km inboard of the Silvia-Pijao Fault ([Fig. 10A](#)). The Peltetec - Silvia Pijao Fault is the western boundary of the Quebradagrande Complex and is considered here to represent the Jurassic-Early Cretaceous continental margin. These early arc magmas assimilated large quantities of continental crust, and are highly enriched in LILE, LREE, and nonradiogenic Nd and Hf isotopes. These rocks were coeval with arc magmatism within southern Peru ([Boekhout et al., 2012](#)). The lack of arc magmatism within Venezuela during 194–209 Ma ([Van der Lelij et al., 2016](#)) suggests it was located more than 400 km from the Pacific active margin, while the inter-American gap had not yet opened.

The arc axis migrated westwards after ~194 Ma, although the rates of extension may have been low because the associated extensional sedimentary rocks were deposited in continental and shallow marine environments ([Cediel, 2018](#)). The westward shift gave rise to a long-lived and continuous

**FIG. 10**

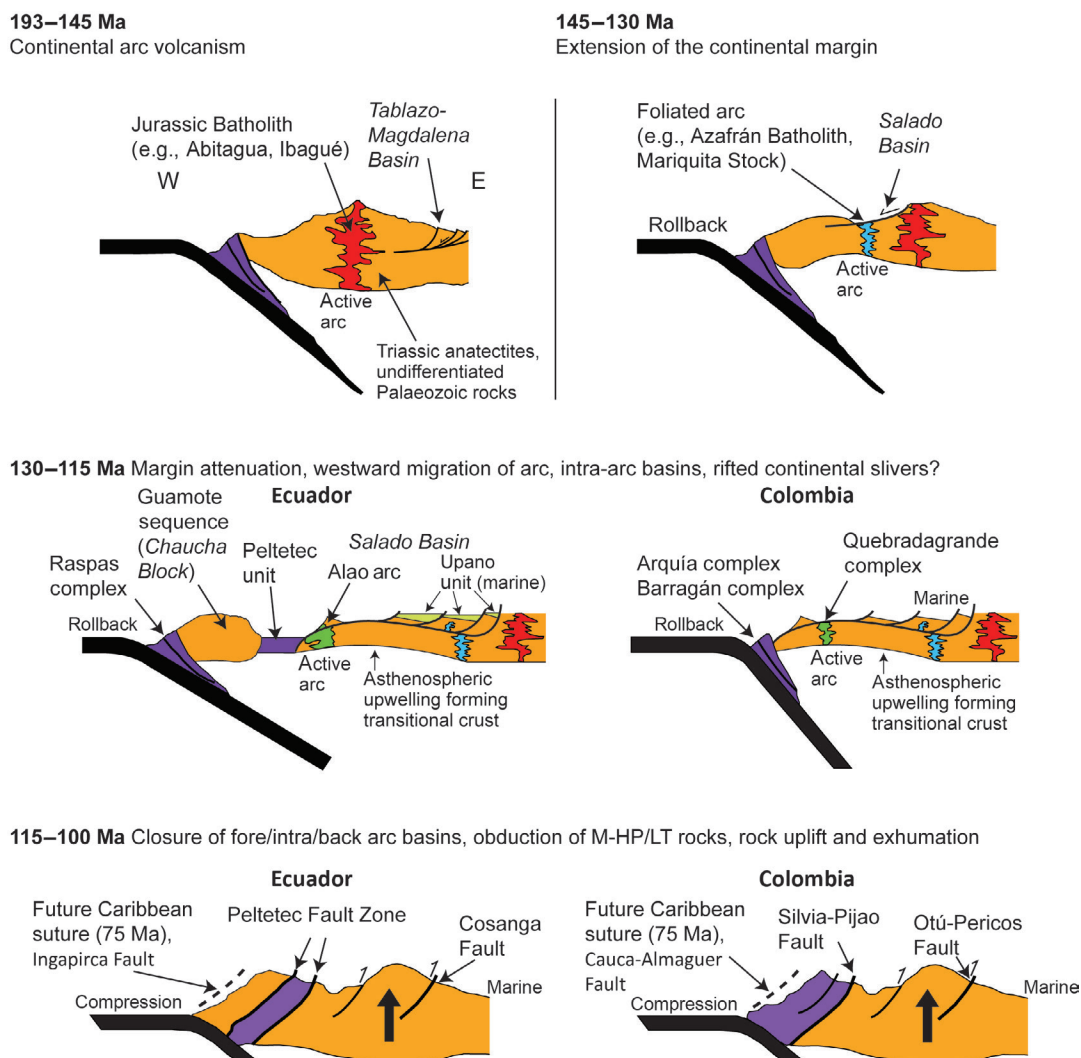
See figure caption on opposite page.

(Fig. 5) calc-alkaline, metaluminous arc (130–193 Ma), which is defined by the Segovia, San Lucas, Ibagué, Mariquita, Rosa Florida, Abitagua, Azafrán, Chinguál, and Zamora batholiths throughout the Cordillera Central of Colombia and Cordillera Real of Ecuador. In addition, other Jurassic plutons are exposed along the western and eastern flanks of the Upper Magdalena Valley in southern Colombia (Fig. 2; Rodriguez et al., 2018) and several volcanic formations (e.g., the Misahualli Fm. in Ecuador; Figs. 10A and 11). These intrusions yield more radiogenic Hf and Nd isotopic compositions (Fig. 8C), and are more metaluminous (Fig. 7B) than during 194–209 Ma, suggesting they are either derived from a more juvenile source, or have assimilated less continental crust. Rodriguez et al., 2018 report that the Jurassic plutons located along the western flank of the Upper Magdalena Valley are older, and geochemically distinct to Jurassic plutons located along the eastern flank. However, our own comparison of their data (Fig. 6B), combined with the assumption that strike-slip displacement has not significantly modified the original arc juxtaposition, does not reveal such a trend. Similarly, major element compositions (Fig. 7) also do not reveal distinct differences in the composition of Jurassic plutons exposed along the flanks of the Upper Magdalena Valley, and other Jurassic intrusions within the cordilleras Central and Real. Rather, a comparison of age and longitude suggests that magmatism during 193–145 Ma was focused in a zone with a width of ~100 km (Figs. 6B and 10A), while the oldest intrusions occur along the eastern flanks of the Cordillera Central (e.g., San Lucas Batholith; Fig. 2). The progressive increase in radiogenic Hf and Nd isotopic compositions during 209–145 Ma, combined with a steady trend from high-K calc-alkaline to calc-alkaline compositions (Fig. 8), suggests that arc magmatism progressively assimilated a smaller proportion of evolved continental crust during 209–145 Ma. This supports the hypothesis that the crust was thinning throughout 209–145 Ma, perhaps during low rates of extension, which was responsible for the significant arc width (~100 km). We further hypothesize that extension was driven by slab retreat that prevailed throughout the Jurassic. The trench - arc distance at various latitudes may have oscillated during 193–145 Ma (e.g., Leal-Mejía et al., 2018) due to short temporal variations in slab dip that typically span ~10 Myr (e.g., Kay et al., 2006), although the geochemical and isotopic data provide a compelling argument for a prevailing extensional regime.

Westward migration of the Middle-Late Jurassic arc axis by 100 km is similar to the quantity measured by Boekhout et al. (2012) and Demouy et al. (2012) in the region of Arequipa (from the city of Arequipa toward the coast), although migration at that location is considered to have started

#### FIG. 10, CONT'D

(A) Subduction zones along western Pangaea during the Jurassic determined using an arc-trench distance of 300 km, and constant slab dip. These subduction zones are derived assuming that the Tahamí Terrane in autochthonous. Paleopositions, plate motion, and reconstructions for Yucatan and central and southern Mexico are taken from Pindell and Kennan (2009), and reconstruction at 189–130 Ma is from their reconstruction for 158 Ma. Black arrows indicate amount of lateral migration of the subduction zone between 194 and 189 Ma (Colombia and Ecuador) and after ~175 Ma (southern Peru). Gray line is present-day coastline, and position of the Nazca Ridge. A, Abitagua Batholith; CC, Cordillera de Carabaya; I, Ibagué Batholith; IB, Illo Batholith; P-SPF, Peltetec-Silvia Pijao Fault (this is the Jurassic-Early Cretaceous paleomargin; Vallejo et al., 2006); S, San Lucas Batholith; Z, Zamora Batholith. (B) Subduction zones and reconstruction of Pindell and Kennan (2009), which assume that the Tahamí Terrane of Colombia is allochthonous, and that the Chaucha Terrane (Litherland et al., 1994) exists. Blue line is a rift axis. C, Chaucha Block; Ch, Chortis Block; T, Tahamí Terrane.

**FIG. 11**

Schematic models for the tectonic evolution of the northwestern South American margin, which fit the geochronological, geochemical, isotopic, thermochronological, and sedimentological data. These models propose that the Jurassic arc axis during 193–145 Ma did not drift. Roll-back starting at 145 Ma caused the arc axes to migrate oceanward and thinned the crust, leading to calk-alkaline and tholeiitic arc magmatism, occasionally T-MORB basalts and marine sedimentary environments. Extension in some parts of the margin may have caused continental slivers to rift away, forming extensive tracts of transitional crust (Peltetec Unit) in intra-arc basins, perhaps accounting for the Guamote Sequence. Compression starting at 120 Ma obducted exhumed M-HP/LT rocks outboard of the Alao and Quebradagrande arcs, and entrained ultramafic and mafic rocks of the Peltetec Unit between those arcs and reaccreted continental slivers.

at ~175 Ma. Migration of the arc axes may be due to either slab steepening and migration relative to the trench, or migration of the trench and subducted slab to the west, extending the margin. This interpretation is consistent with (i) [Sempere et al. \(2002\)](#), who utilize sedimentary facies to demonstrate that the margin of Arequipa was extending throughout the Jurassic, and [Boekhout et al. \(2012\)](#) report subsidence rates of ~3.5 km/My, (ii) Jurassic back arc magmatism through thin continental crust (173–195 Ma; [Miskovic et al., 2009](#)) in the Cordillera de Carabaya, southern Eastern Cordillera of Peru, and (iii) reconstructions of [Pindell and Kennan \(2009\)](#), who draw rift zones extending from Central Peru toward northern Colombia throughout the Jurassic period ([Fig. 10B](#)). Jurassic extensional basins are recognized to the east of the Jurassic intrusions, which are characterized by grabens with varying rates of subsidence (e.g., Bogota Basin) in Colombia ([Toussaint and Restrepo, 1994](#)). In general, a Triassic-Barremian syn-rift megasequence in Colombia was dominated by continental clastic sediments (e.g., Tablazo-Magdalena Basin; [Fig. 11](#); [Cooper et al., 1995](#)). Within Ecuador, subsidence gave rise to a 2000-m-thick sequence of Sinamurian limestones and sandstones of the Santiago Fm. ([Litherland et al., 1994](#)) in the southern Sub-Andean Zone of Ecuador ([Fig. 1](#)), and in northern Peru ([Jaillard et al., 1990](#)).

The oldest crystallization ages at any given location ([Fig. 5A](#)) show a general younging trend from northern Colombia to southern Ecuador, suggesting the onset of subduction may have been diachronous north of the Huancabamba Deflection (see also the compilation in [Leal-Mejía et al., 2018](#)). The lack of continental arc rocks older than ~181 Ma south of ~2.5°S ([Fig. 5](#)) suggests subduction may have initially started in northern Colombia, and extended southwards at ~181 Ma. Furthermore, the extension of Jurassic arc magmatism to the Late Jurassic is only abundant in the northern Ibagué Batholith ([Fig. 5](#)). These observations may suggest that distinct episodes of Jurassic magmatism occurred during 209–145 Ma, which define specific groups of intrusive rocks. [Leal-Mejía et al. \(2018\)](#) provide a detailed description of possible intrusions grouped according to their zircon U-Pb concordia ages.

Arc magmatism in Peru started as early as 216 Ma ([Fig. 10A](#)), and occurred until <135 Ma, as recorded by the Chocolate Fm. and the Ilo Batholith ([Boekhout et al., 2012](#)). Calc-alkaline, metaluminous arc intrusions along coastal Arequipa were accompanied by coeval, alkali back-arc magmatism in the Cordillera de Carabaya during 173–195 Ma ([Fig. 10A](#); [Miskovic et al., 2009](#)). This time period broadly corresponds with a westward jump of the arc axis in the Northern Andes during 194–189 Ma, although coeval arc-back arc relationships have not been found in the Northern Andes. Clearly, the potentially diachronous onset of arc magmatism in the Northern Andes cannot be extended across the Huancabamba Deflection.

## 5.2 The tectonic setting during the Early Cretaceous (145–115 Ma)

The compiled zircon U-Pb dates, geochemistry, and isotopic data clearly show that I-type, metaluminous, high-SiO<sub>2</sub> (>75%; [Fig. 7](#)) arc rocks formed the Azafrán and Chinguál Batholiths, parts of what is mapped as the Zamora Batholith (granodiorite 09RC43), and the Mariquita Stock during 144–130 Ma (Table 1 in the online version at <https://doi.org/10.1016/B978-0-12-816009-1.00009-5;Figs. 2, 3, and 11>). These units are exposed to the west of the older arc intrusions in Ecuador, are bound against the Cosanga Fault ([Fig. 6](#)) to their east, and exhibit a weak-to-strong foliation ([Pratt et al., 2005](#)) that is mainly absent (except for local fault foliation) in the latest Triassic to Jurassic intrusions. The Hf and Nd isotopic compositions ([Fig. 8](#)) indicate that they crystallized from melts that were more juvenile

than the older, unfoliated Jurassic intrusions and they are considered by Spikings et al. (2015) to have erupted through thinned crust (Fig. 11). This interpretation is consistent with Pratt et al. (2005) who suggest the foliations formed during pure shear, and Litherland et al. (1994) who suggest that magmatism within the “Salado Terrane” occurred within a marginal basin (Fig. 11). U-Pb dates of detrital zircons in sandstones of the Upano Unit suggest this marginal basin formed after 143 Ma, which is consistent with the crystallization ages of the Azafrán and Chinguál plutons (Spikings et al., 2015). We suggest that the Cosanga Fault originated within an extensional system, and extensional rates increased along the northwestern Pacific margin of South America at ~144 Ma. Extension during 144–130 Ma coincides with (i) high sedimentation rates in Early Cretaceous rifts located along the eastern flank of the Eastern Cordillera (Mora et al., 2008, 2009; Teson et al., 2013), and (ii) extension of the basement of the Oriente Basin in Ecuador (Balkwill et al., 1995) and in northern Peru (Jaillard et al., 1990).

Mafic, calc-alkaline to tholeiitic volcanic rocks of the Alao and Quebradagrande Complexes are preserved to the west of the Azafrán and Chinguál Batholiths, and west of an uplifted core (Pratt et al., 2005) of Paleozoic basement and Triassic migmatites (Fig. 11). Major trace element and REE compositions suggest these formed within arcs (Fig. 9), although some samples yield an affinity with MORB. The volcanic rocks are located outboard of the Jurassic intrusions (Fig. 6B), and yield juvenile Hf and Nd isotopic compositions and depleted trace elements relative to the Jurassic intrusions (Fig. 8). Scant geochronological data suggest the volcanic rocks within the Quebradagrande Unit erupted at ~114 Ma, while the volcanoclastic rocks were deposited after ~149 Ma (Spikings et al., 2015). No accurate age estimates of the Alao arc are available although sedimentation could have occurred after ~164 Ma (Spikings et al., 2015). K/Ar dates of  $115 \pm 12$  Ma and  $142 \pm 36$  Ma suggest it could be coeval with the Quebradagrande Complex. This tectonic correlation is supported by its outboard position relative to the Paleozoic basement, Triassic anatectites, and Jurassic intrusions, and we tentatively assign an Early Cretaceous age to the Alao arc.

The Alao Arc hosts large volumes of quartz-zircon-tourmaline rich arenites (Cochrane et al., 2014b), and U-Pb ages of detrital zircons (Spikings et al., 2015) reveal a derivation from cratonic South America. Therefore, the Alao Arc is interpreted to have formed above an east-dipping subduction zone along the thinned fringe of a continental margin, giving rise to isotopically juvenile, mafic volcanic rocks (Cochrane et al., 2014b; Fig. 11). Extension was sufficient to form MORB-like rocks with tholeiitic signatures above the subduction zone. Alternatively, the tholeiitic basalts may form part of the Peltetec Unit (Fig. 6), and were structurally emplaced against the calc-alkaline rocks during subsequent compression. This interpretation differs from that of Litherland et al. (1994), who draw the Alao Arc as an intraoceanic Middle Jurassic arc, which is inconsistent with the presence of abundant Precambrian zircons. Similarly, the volcanic rocks of the Quebradagrande Complex are associated with sedimentary rocks (Abejorral Fm.; e.g., Gomez-Cruz et al., 1995) that host abundant quartz, and Nivia et al. (2006) interpreted this sequence as a thinned marginal basin along a continental margin (Fig. 10). Villagomez et al. (2011), Spikings et al. (2015), and Jaramillo et al. (2017) suggest the arc rocks erupted through highly attenuated continental crust because (i) some basalts yield geochemical signatures that approach seamounts (T-MORB), (ii) most volcanic rocks erupted in submarine conditions, and (iii) no continental detritus is found to the west of the Quebradagrande Complex. Pindell and Kennan (2009) draw the Quebradagrande Arc as an oceanic arc above an east-dipping subduction zone until 125 Ma, although this date is not based on robust geochronological evidence from northwestern South America.

The simplest explanation for the geochemical, isotopic, and geochronological trends obtained from the Jurassic and Early Cretaceous igneous rocks is that they formed above the same east-dipping subduction zone, which was retreating oceanward during 209–194 Ma, and after ~145 Ma until ~114 Ma (E.g., Spikings et al., 2015; Fig. 11). Extension of the continental crust during ~130–114 Ma was sufficient

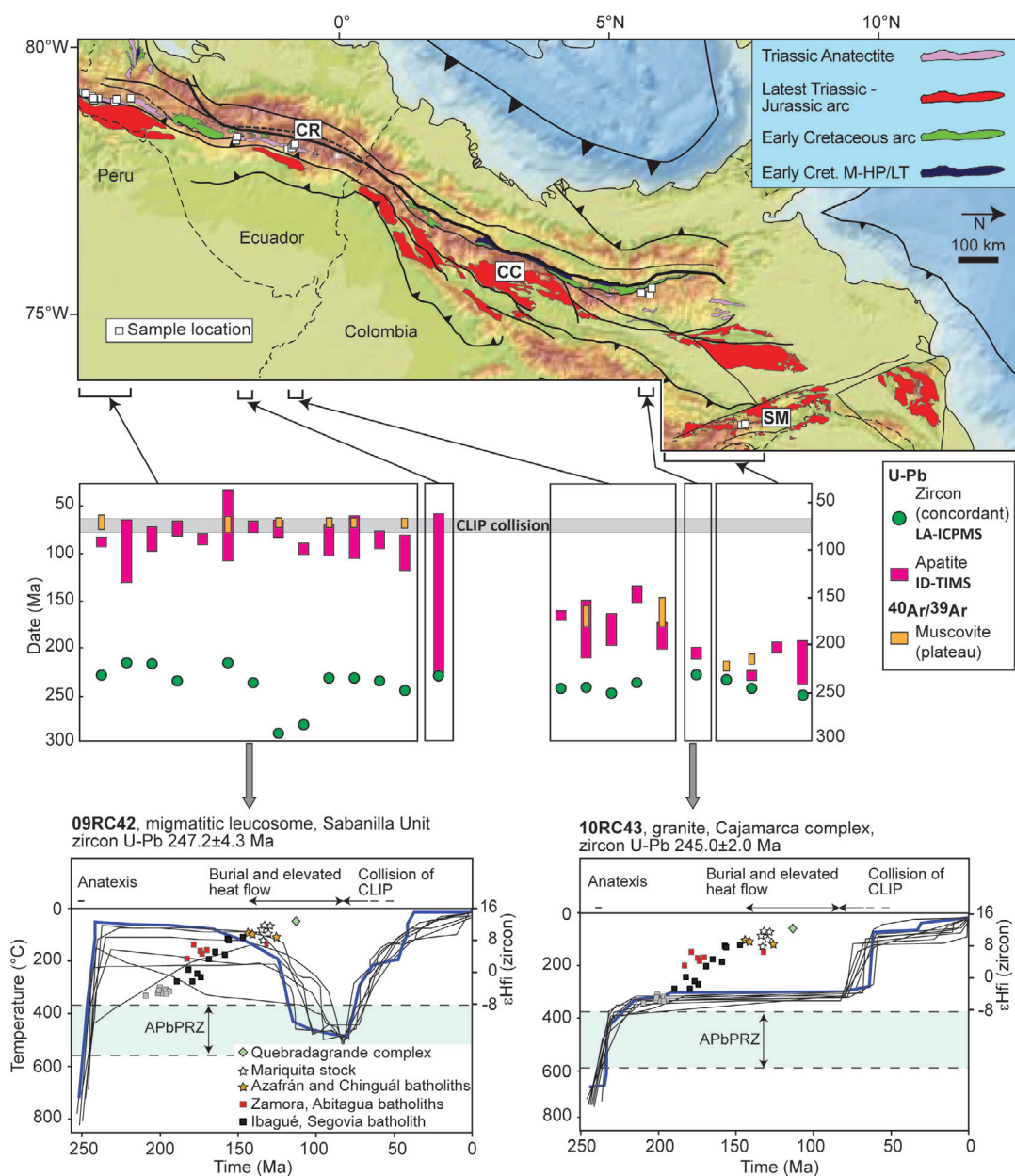
to generate mafic magmas with T-MORB geochemical characteristics and marine environments, which are found intercalated within the Alao and Quebradagrande sequences. [Kennan and Pindell \(2009\)](#) refer to this extensional feature as the Colombian Marginal Seaway. This time period (Early Cretaceous) corresponds with heating of Triassic leucosomes within the southern Cordillera Real ([Fig. 12](#)) to temperatures of up to ~500°C ([Cochrane et al., 2014c; Spikings et al., 2015; Paul et al., 2018](#)), which was synchronous with a significant increase in  $\epsilon\text{HF}_i$  (zircon) in the magmatic rocks. Heating is interpreted to be a consequence of sedimentary burial (e.g., Salado Basin of Ecuador) during extension, combined with an increase in geothermal gradients. The maximum temperatures reached during reheating in the Jurassic-Early Cretaceous diminishes toward the north ([Fig. 12](#); e.g., northern Colombia), presumably due to a reduction in the amount of extension, burial, and heat flow ([Paul et al., 2018](#)). Some faulted units (e.g., south of the Ibagué Fault in the Cordillera Central; [Villagomez and Spikings, 2013](#)) were cooling at ~140 Ma ([Fig. 13](#)), perhaps because they were exhumed during extension.

This interpretation is similar to that of [Toussaint and Restrepo \(1994\)](#), [Cooper et al. \(1995\)](#), [Sarmiento-Rojas et al. \(2006\)](#), and [Pindell and Kennan \(2009\)](#) who suggest that the rocks of the Eastern Cordillera of Colombia ([Fig. 1](#)) underwent back-arc extension (NNE-SSW extensional axis; e.g., [Mora et al., 2006](#)), during the Cretaceous, associated with an arc that formed rocks, which are now exposed within the Cordillera Central (Quebradagrande Complex). [Vasquez and Altenberger \(2005\)](#) and [Vasquez et al. \(2010\)](#) report that gabbroic intrusions exposed in the Eastern Cordillera ([Fig. 1](#)) formed within a rift setting during 135 and 121 Ma (Table 1 in the online version at <https://doi.org/10.1016/B978-0-12-816009-1.00009-5>). The MORB and OIB-type chemistry of these rocks ([Vasquez et al., 2010](#)) suggests that back-arc extension was significant.

The Guamote Sequence of [Litherland et al. \(1994\)](#) ([Fig. 6](#); Chaucha Block) does not host any magmatic rocks, and is composed of metasedimentary rocks that were deposited after 155 Ma ([Spikings et al., 2015](#)). The Braziliiano and Sunsas aged U-Pb ages of detrital zircons show that the sediments were derived from cratonic South America. Furthermore, their detrital age signature is indistinguishable from that obtained from arenites within the Alao Arc, Quebradagrande Complex and the Upano Unit ([Spikings et al., 2015](#)). The Guamote Sequence is currently separated from the Alao Arc by ultramafic-mafic rocks of the Peltetec Complex, although it is not unreasonable to suggest it once formed a part of the South American Margin, and was emplaced either by (i) strike-slip displacement from more southern latitudes, or by (ii) rifting away from north-western South America, followed by reaccretion ([Fig. 11](#)).

[Litherland et al. \(1994\)](#) suggest that prior to 140 Ma, continental crust of the Chaucha Block lay outboard of a west-facing island arc (Alao Arc), which was separated from South America by oceanic crust that was subducting beneath South America, forming the Azafrán Pluton. Subsequently, the same authors suggest that these are terranes that collided together during 140–120 Ma, during the compressive Peltetec Event. Similarly, [Villagomez and Spikings \(2013\)](#) suggest that the collision of a series of seamounts or oceanic plateau blocked the Jurassic subduction zone, terminating the Jurassic arc, and that a new subduction zone formed outboard of the hypothetical plateau, forming the west-facing Quebradagrande Arc. However, the data compiled here suggest that (i) arc magmatism during the Jurassic-Early Cretaceous formed above a single subduction zone, (ii) the Quebradagrande Complex was a continental arc that erupted through thinned continental crust, and (iii) extension prevailed during the Early Cretaceous. No evidence exists for a Jurassic oceanic plateau within Colombia or Ecuador. Furthermore, [Spikings et al. \(2015\)](#) do not consider these to represent terranes. Rather, they are para-autochthonous to South America.

The Arquía, Barragán, and Raspas complexes are considered to be equivalent because (i) they are located in similar structural positions, outboard of Triassic anatectites, and volcanic arc rocks, (ii) they

**FIG. 12**

See figure caption on next page.

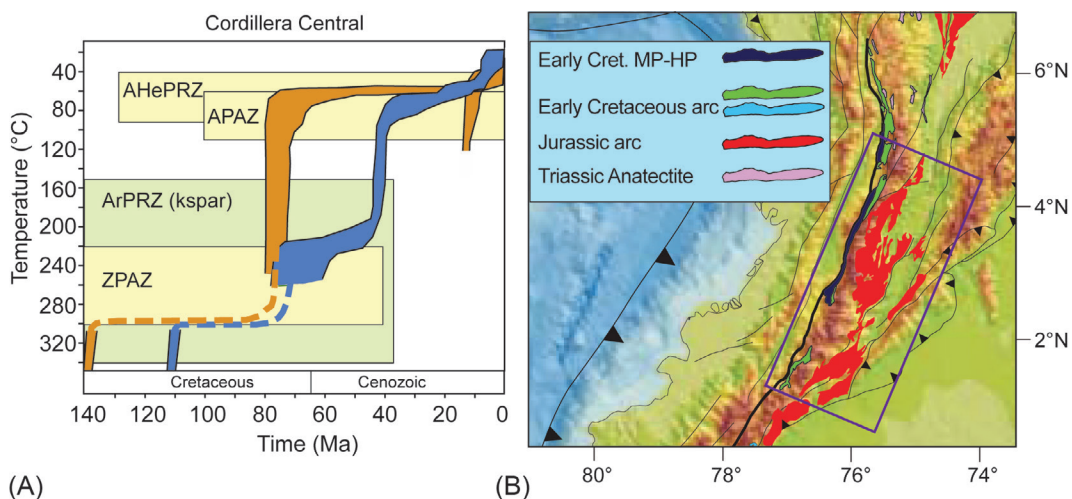
are composed of basalts and gabbros that have been metamorphosed to varying degrees under M-HP/LT conditions, (iii) they yield peak metamorphic and retrogression dates that are similar, and (iv) they yield MORB-seamount geochemical signatures. The Raspas Complex now forms part of the para-autochthonous Amotape Terrane, which detached from rocks that are now exposed in the Cordillera Real. The Raspas Complex hosts HP-LT rocks of oceanic plateau and MORB affinity (Arculus et al., 1999; Bosch et al., 2002; John et al., 2010), which were exhumed following peak metamorphism at 130–126 Ma (John et al., 2010). Geochemical and isotopic compositions also suggest the Barragán (HP-LT) and Arquía (MP-LT) units originated as MORB and seamounts (Bustamante et al., 2012), while their  $^{40}\text{Ar}/^{39}\text{Ar}$  dates suggest they were exhuming and cooled below  $\sim 400^\circ\text{C}$  during 120–112 Ma. We consider these units to have been metamorphosed within the same subduction zone, which was exhumed to variable degrees along-strike of northwestern South America (Fig. 11). Exhumation could have been triggered by forced return flow (Gerya et al., 2002), which may have occurred during a compressive event, combined with the inherent buoyancy of oceanic plateau rocks relative to MOR-derived lithosphere.

Rifting of northwestern South America during the Early Cretaceous may have been sufficient to detach continental slivers (e.g., the Chaucha Block in Ecuador), and we suggest that the greenschist facies ultramafic-mafic rocks of the Peltetec Complex formed during advanced continental rifting as E-MORB crust (Fig. 11). The Peltetec Complex has not been metamorphosed in a subduction zone, and its current structural position between the Guamote Sequence and the Alao Arc in Ecuador indicates they were obducted during a compressional event. Their  $^{40}\text{Ar}/^{39}\text{Ar}$  dates suggest they formed at  $\sim 134$  Ma (Spikings et al., 2015), and hence they formed before the subduction channel that hosted the Arquía, Barragán, and Raspas complexes was exhumed.

Early Cretaceous extension caused greater amounts of reheating of the Triassic crystalline basement exposed in the Cordillera Real, in southern Ecuador (Fig. 12), compared to similar rocks in the Cordillera Central of Colombia. This was interpreted by Paul et al. (2018) to reflect greater amounts of crustal thinning and extension in southern Ecuador, which corroborates the presence of transitional crust (Peltetec Unit) and the detachment of para-autochthonous continental slivers (Chaucha Block) in Ecuador, which are not recognized in Colombia.

#### FIG. 12, CONT'D

Along-strike variations of U-Pb concordia dates (zircon),  $^{238}\text{U}/^{206}\text{Pb}$  dates (apatite; grain radii of  $\sim 50$  and  $100\mu\text{m}$ ; ID-TIMS), and  $^{40}\text{Ar}/^{39}\text{Ar}$  plateau dates (muscovite) from Triassic lithologies (Tres Lagunas Granite, Sabanilla Migmatite, and Amphibolite). Data are from Paul et al. (2018). The gray bar indicates the timing of the collision and accretion of the Caribbean Large Igneous Province (CLIP; oceanic plateau and overlying intraoceanic arc), determined using various low-T thermochronometers, sedimentological and paleomagnetic evidence (Vallejo et al., 2006; Luzieux et al., 2006; Spikings et al., 2010).  $^{238}\text{U}/^{206}\text{Pb}$  and  $^{40}\text{Ar}/^{39}\text{Ar}$  dates are clearly younger toward the south, with a transition zone in northern Ecuador. Time ( $t$ )-Temperature ( $T$ ) plots are shown for 2 leucosomes from southern Ecuador (09RC42; Cochrane et al., 2014c) and northern Colombia (10RC43; Spikings et al., 2015), which satisfy the apatite U-Pb data. The  $t$ - $T$  paths were determined by inverting the U-Pb dates and grain sizes, using the diffusivity and activation energy of diffusion of Pb in apatite (Cherniak et al., 1991). The blue line is the best-fit solution.  $\epsilon\text{Hf}_t$  (zircon) are also shown for the latest Triassic-Early Cretaceous igneous rocks studied here (Table 1 in the online version at <https://doi.org/10.1016/B978-0-12-816009-1.00009-5>), and reveal steadily increasing values throughout the Jurassic to the middle of the Cretaceous, which accompanied reheating. APbPRZ: Apatite Pb Partial Retention Zone.

**FIG. 13**

Time-temperature solutions (A) for autochthonous rocks of the southern and central Central Cordillera of Colombia, highlighted by the purple rectangle in (B), obtained by inverse modeling of apatite fission track age and length data, and weighted mean (U-Th)/He dates and grain size data (calculated using the weighted mean of the diffusion lengths). The models are extrapolated to the Ar Partial Retention Zone (ArPRZ) for alkali feldspar and Zircon (fission track) Partial Annealing Zone (ZPAZ), where appropriate. Models and data are taken from [Villagomez and Spikings \(2013\)](#).

### 5.3 Compression during the Early Cretaceous

Dense mineral assemblages and detrital zircon fission track dates with very short lag-times suggest that rocks deposited within the Upper Magdalena Valley (Fig. 1; [Vergara and Prössl, 1994](#); [Sarmiento and Rangel, 2004](#)) and Oriente ([Ruiz et al., 2007](#); [Martin-Gombojav and Winkler, 2008](#)) basins during 120–115 Ma were derived from an exhuming cordillera located to the west. [Restrepo et al. \(2009\)](#) suggest that Aptian-middle Albian sandstones of the Abejorral Fm., which are located along the western flank of the Cordillera Central, were derived from a proto-Central Cordillera to the east. Time-Temperature paths for some faulted blocks suggest they cooled rapidly at 117–107 Ma (Fig. 13). [Villagomez et al. \(2011\)](#) interpret these data as evidence for compression, which exhumed some fault blocks, forming a proto-Cordillera Central. This is consistent with an unconformity that separates the Hollin and Chapiza sedimentary formations in the western Oriente Basin of Ecuador. The youngest detrital zircon in the basal arenites of the Hollin yields a zircon U/Pb date of ~116 Ma ([Romero, 2018](#); ages of populations are not provided, nor are the uncertainties), while the underlying volcanoclastic strata of the Chapiza Fm. yield a Valanginian age ([Ordonez et al., 2006](#)). This time period coincides with the timing of retrogression of the east-dipping subduction zone during exhumation, and compression at this time obducted blueschists and eclogites of the Raspas, Arquía, and Barragán complexes onto the South American margin. Compression may have occurred due to an increase in the convergence rates of the oceanic Caribbean Plate ([Kennan and Pindell, 2009](#)) and South America, as a consequence of the opening of the South Atlantic, which started at ~120 Ma ([Eagles, 2007](#)). Detrital zircon fission track dates from the Oriente Basin of Ecuador

(Fig. 1; Ruiz et al., 2004) suggest a second compressive event may have occurred within Ecuador at ~100 Ma, which would be coeval with compression in Peru (Megard, 1984).

Maresch et al. (2009) report metamorphic zircon dates of 116–106 Ma from anatectites within HP-LT metagabbros at La Rinconada, Margarita Island (southern Caribbean). Those rocks are interpreted as back-arc basin crust that was subducted and retrogressed during 116–106 Ma. The coincidence in the timing of metamorphism in northwestern South America and Margarita Island suggests they may have formed in the same tectonic setting. However, Maresch et al. (2009) suggest the HP-LT rocks at Margarita Island formed on a west-dipping slab of continental back-arc crust. The same arc polarity is shown by Pindell et al. (2005) at 119 Ma, although Pindell and Kennan (2009) suggest that the polarity of the subduction zone flipped during 125–120 Ma, during the transition from their Trans-American Arc, to the Caribbean Arc, and the separation of North America from Gondwana. However, it is difficult to account for the outboard position of M-HP/LT metamorphic rocks relative to the Alao and Quebradagrande arcs within an east-facing arc system, and the simplest explanation of the very large amount of data obtained from Jurassic and Early Cretaceous rocks of the northern Andes suggest that subduction was east dipping beneath South America.

## 6 Conclusions

1. Metaluminous, I-type arc magmatism commenced in northwestern South America at ~209 Ma, due to east-dipping subduction of the Farallon Plate. The arc axis migrated oceanward at ~194 Ma, and formed a long-lived continental arc during 193–145 Ma, which spanned a width of ~100 km, and was accompanied by progressive thinning of the continental crust. The trench-arc distance may have oscillated during this time period as a result in variations in slab dip. Coeval arc magmatism along the Peruvian margin (~216–135 Ma) started to migrate oceanward at ~175 Ma, resulting in coeval arc and back-arc rocks. Lithospheric thinning is considered to be a result of prevailing slab retreat along the western margin of South America, which caused the continental margin to extend, thinning the continental crust and generating progressively more isotopically juvenile arcs. The onset of latest Triassic-Jurassic subduction beneath Colombia and Ecuador becomes younger toward the south, resulting in arc magmatism after ~181 Ma, south of 2.5°S. although this trend cannot be extended toward southern Peru, across the Huancabamba Deflection. Late Jurassic arc magmatism is only abundant in the northern Ibagué Batholith, and thus distinct episodes of Jurassic magmatism may have occurred during 209–145 Ma, which formed geographic groups of intrusive rocks.
2. Trench retreat of the east-dipping-subduction zone accelerated along northwestern South America at ~144 Ma, and extension during 144–115 Ma formed syn-tectonic granitoid intrusions within Ecuador, attenuated the continental margin forming thin intra-arc basins (e.g., the Salado Basin of Ecuador) characterized by transitional crust, and resulted in an oceanward migration of the arc axes, which became progressively more isotopically juvenile and geochemically depleted. Arc rocks of the Quebradagrande Complex and Alao arc erupted through thin continental crust during the Early Cretaceous within a marine environment. Rapid extension may have rifted some narrow continental slivers (e.g., the Chaucha Block) from the margin. Back-arc magmatism is sporadically preserved within the Eastern Cordillera of Colombia (136–121 Ma). Highly oblique and sinistral convergence directions between the Peruvian margin and the Farallon Plate lead to a magmatic gap in Peru during ~135–115 Ma.

3. Along-strike variation in apatite U-Pb dates obtained from Triassic leucosomes reveals increased temperatures during reheating in the Early Cretaceous. Reheating is interpreted to be a consequence of burial and increased heat flow during extension, corroborating the interpretations obtained from the geochronological, geochemical, and isotopic data from the Jurassic-Early Cretaceous igneous rocks. Larger amounts of reheating are recorded by the Triassic crystalline basement in southern Ecuador, compared to northern Ecuador and Colombia. This is interpreted to reflect greater amounts of extension in the Early Cretaceous, which perhaps accounts for the existence of transitional crust (Peltetec Unit) inboard of para-autochthonous continental slivers (Chaucha Block).
4. The distribution and composition of sedimentary rocks, combined with detrital thermochronology, suggests that the margin of northwestern South America was placed under compression at ~115 Ma. Compression of the attenuated, weak, hot crust juxtaposed arc rocks with transitional crust, forming a proto-cordillera, which supplied detritus toward the fore- and backarc. M-HP/LT rocks are faulted against the western margin of these compressed sequences and represent a subduction channel that started to exhume from peak eclogitic conditions at 130–126 Ma. These eclogites and blueschists retrogressed through ~400°C at 120–112 Ma, and it is likely that they were obducted onto the margin during compression that started at ~115 Ma. These rocks originally formed parts of the same slab, and varying trench-parallel metamorphic facies reflect exhumation from varying depths. Models, which invoke west-dipping slabs after 125 Ma, do not account for the spatial juxtaposition of M-HP/LT rocks and their associated arcs.

## Acknowledgments

We thank Lluis Carlos Mantilla, Andreas Kammer, Alejandro Beltran, Ecopetrol S.A., and Andres Mora for their assistance during field work in Colombia. Bernardo Beate, Arturo Egüez, Etienne Jaillard, Alfredo Buitron, Byron Pelicita, and Luis Lopez are thanked for their assistance in the field in the cordilleras of Ecuador. Reviews by Andres Mora and an anonymous reviewer improved the content of this study. This work was financed by the Swiss National Science Foundation grants 200020\_134443 and 200020\_146332, which were awarded to RS.

## Appendix: Supplementary material

Supplementary material related to this chapter can be found on the accompanying CD or online at <https://doi.org/10.1016/B978-0-12-816009-1.00009-5>.

## References

- Alvarez, J.A., 1983. Geología de la Cordillera Central y el occidente colombiano y petroquímica de 10 s intrusivos granitoides Mesocenozoicos. vol. 26. Boletín Geological INGEOMINAS, Bogota, Colombia.
- Arculus, R.J., Lapierre, H., Jaillard, E., 1999. Geochemical window into subduction and accretion processes: Raspas metamorphic complex, Ecuador. *Geology* 27, 547–550.

- Aspden, J.A., McCourt, W.J., Brook, M., 1987. Geometrical control of subduction-related magmatism: the Mesozoic and Cenozoic plutonic history of Western Colombia. *J. Geol. Soc.* 144, 893–905.
- Baldock, M.W., 1982. Geology of Ecuador, explanatory bulletin of the national map of the Republic of Ecuador, scale 1:1,000,000. Rev. Dir. Gen. Minas Ecuador 11, 54 pp.
- Balkwill, H.R., Paredes, F.I., Rodriguez, G., Almeida, J.P., 1995. Northern part of Oriente Basin, Ecuador: reflection seismic expression of structures. In: Tankard, A.J., Suarez, R., Welsink, H.J. (Eds.), *Petroleum Basins of South America*: American Association of Petroleum Geologists. vol. 62, pp. 559–571.
- Batchelor, R.A., Bowden, P., 1985. Petrogenetic interpretation of granitoid rock series using multicationic parameters. *Chem. Geol.* 48, 43–55.
- Bayona, G., Rapalini, A., Costanzo-Alvarez, V., 2006. Paleomagnetism in Mesozoic rocks of the Northern Andes and its implications in Mesozoic Tectonics of Northwestern South America. *Earth Planets Space* 58, 1255–1272.
- Bayona, G., Jimenez, G., Silva, C., Cardona, A., Montes, C., Roncancio, J., Cordani, U., 2010. Paleomagnetic data and K-Ar ages from Mesozoic units of the Santa Marta massif: a preliminary interpretation for block rotation and translations. *J. S. Am. Earth Sci.* 29, 817–831.
- Boekhout, F., Spikings, R., Sempere, T., Chiaradia, M., Ulianov, A., Schaltegger, U., 2012. Mesozoic arc magmatism along the southern Peruvian margin during Gondwana breakup and dispersal. *Lithos* 146–147, 48–64.
- Boekhout, F., Roberts, N.M.W., Gerdes, A., Schaltegger, U., 2013. A Hf-isotope perspective on continent formation in the south Peruvian Andes. *Geol. Soc. Lond. Spec. Publ.* 389, <https://doi.org/10.1144/SP389.6>.
- Bosch, D., Gabriele, P., Lapierre, H., Malfiere, J.-L., Jaillard, E., 2002. Geodynamic significance of the Raspas metamorphic complex (SW Ecuador): geochemical and isotopic constraints. *Tectonophysics* 345, 83–102.
- Bourgois, J., Toussaint, J.-F., Gonzales, H., Azema, J., Calle, B., Desmet, A., Murcia, L.A., Acevedo, A.P., Parra, E., Tournon, J., 1987. Geological history of the Cretaceous ophiolitic complexes of Northwestern South America (Colombian Andes). *Tectonophysics* 143, 307–327.
- Bristow, C.R., 1973. Guide to the Geology of the Cuenca Basin, Southern Ecuador. Ecuadorian Geological and Geophysical Society, Quito.
- Bustamante, A., 2008. Geobarometria, geoquímica, geocronologia e evolução tectônica das rochas de fácies xisto azul nas áreas de Jambaló (Cauca) e Barragán (Valle del Cauca), Colômbia. (PhD Thesis). Instituto de Geociências, Universidade de São Paulo, Brasil, p. 179.
- Bustamante, C., Cardona, A., Bayona, G., Mora, A., Valencia, V., Gehrels, G., Vervoort, J., 2010. U-Pb LA-ICP-MS geochronology and regional correlation of Middle Jurassic intrusive rocks from the Garzón Massif, Upper Magdalena Valley and Central Cordillera, southern Colombia. *Bol. Geol.* 32, 93–109.
- Bustamante, A., Juliani, C., Hall, C.M., Essene, E.J., 2011.  $^{40}\text{Ar}^{39}\text{Ar}$  ages from blueschists of the Jambaló region, Central Cordillera of Colombia: implications on the styles of accretion in the Northern Andes. *Geol. Acta* 9, 351–362.
- Bustamante, A., Juliani, C., Essene, E.J., Hall, C.M., Hyppolito, T., 2012. Geochemical constraints on blueschist-facies rocks of the Central Cordillera of Colombia: the Andean Barragán region. *Int. Geol. Rev.* 54, 1013–1030.
- Bustamante, C., Archanjo, C.J., Cardona, A., Vervoort, J.D., 2016. Late Jurassic to Early Cretaceous plutonism in the Colombian Andes: a record of long-term arc maturity. *Geol. Soc. Am. Bull.* 128, 1762–1779.
- Castro, A., Moreno-Ventas, I., Fernández, C., Vujovich, G., Gallastegui, G., Heredia, N., Martino, R.D., Becchio, R., Corretgé, L.G., Díaz-Alvarado, J., García-Arias, M., Liu, D.-Y., 2011. Petrology and SHRIMP U-Pb zircon geochronology of Cordilleran granitoids of the Bariloche area, Argentina. *J. S. Am. Earth Sci.* 32, 508–530.
- Cediel, F., 2018. Phanerozoic orogens of northwestern South America: Cordilleran-type orogens. Taphrogenic tectonics. The Maracaibo Orogenic Float. The Chocó-Panamá Indenter. In: Cediel, F., Shaw, R.P. (Eds.), *Geology and Tectonics of Northwestern South America*. Frontiers in Earth Sciences, [https://doi.org/10.1007/978-3-319-76132-9\\_1](https://doi.org/10.1007/978-3-319-76132-9_1).
- Cherniak, D.J., Lanford, W.A., Ryerson, F.J., 1991. Lead diffusion in apatite and zircon using ion implantation and Rutherford Backscattering techniques. *Geochim. Cosmochim. Acta* 55, 1663–1673.

- Chiaradia, M., Vallance, J., Fontboté, L., Stein, H., Schaltegger, U., Coder, J., Richards, J., Villeneuve, M., Gendall, I., 2009. U-Pb, Re-Os and  $^{40}\text{Ar}/^{39}\text{Ar}$  geochronology of the Nambija Au-skarn and Pangui porphyry Cu deposits, Ecuador: implications for the Jurassic metallogenic belt of the northern Andes. *Mineral. Deposita* 44, 371–387.
- Cochrane, R., Spikings, R., Gerdes, A., Ulianov, A., Mora, A., Villagómez, D., Putlitz, B., Chiaradia, M., 2014a. Permo-Triassic anatexis, continental rifting and the disassembly of western Pangaea. *Lithos* 190–191, 383–402.
- Cochrane, R., Spikings, R., Gerdes, A., Winkler, W., Ulianov, A., Mora, A., Chiaradia, M., 2014b. Distinguishing between in-situ and accretionary growth of continents along active margins. *Lithos* 202–203, 382–395.
- Cochrane, R., Spikings, R.A., Chew, D., Wotzlaw, J.-F., Chiaradia, M., Tyrell, S., Schaltegger, U., Van der Lelij, R., 2014c. High temperature ( $>350^\circ\text{C}$ ) thermochronology and mechanisms of Pb loss in apatite. *Geochim. Cosmochim. Acta* 127, 39–56.
- Collins, W.J., Belousova, E.A., Kemp, A.I.S., Murphy, J.B., 2011. Two contrasting Phanerozoic orogenic systems revealed by hafnium isotope data. *Nat. Geosci.* 4, 333–337.
- Colmenares, F., 2007. Evolución Geohistorica de la Sierra Nevada de Santa Marta. Internal report No. PS 025-06, 1221, INGEOMINAS.
- Cooper, B., Addison, F.T., Alvarez, R., Coral, M., Graham, R.H., Hayward, A.B., Howe, S., Martinez, J., Naar, J., Peñas, R., Pulham, A.J., Taborda, A., 1995. Basin development and tectonic history of the Eastern Cordillera and Llanos Basin Colombia. *Am. Assoc. Pet. Geol. Bull.* 79, 1421–1443.
- De Haller, A., Corfu, F., Fontboté, L., Schaltegger, U., Barra, F., Chiaradia, M., Frank, M., Alvarado, J.Z., 2006. Geology, geochronology, and Hf and Pb isotope data of the Raúl-Condestable iron oxide-copper-gold deposit, Central Coast of Peru. *Econ. Geol.* 101, 281–310.
- Demouy, S., Paquette, J.-L., Blanquat, M.d.S., Benoit, M., Belousova, E.A., O'Reilly, S.Y., García, F., Tejada, L.C., Gallegos, R., Sempere, T., 2012. Spatial and temporal evolution of Liassic to Paleocene arc activity in southern Peru unravelled by zircon U-Pb and Hf in-situ data on plutonic rocks. *Lithos* 155, 183–200.
- Eagles, G., 2007. New angles on South Atlantic opening. *Geophys. J. Int.* 168, 353–361.
- Feininger, T., Bristow, C.R., 1980. Cretaceous and Paleogene geologic history of coastal Ecuador. *Geol. Rundsch.* 69, 849–874.
- Feininger, T., Silberman, M.L., 1982. K-Ar geochronology of basement rocks on the northern flanks of the Huanca Bamba Deflection, Ecuador. In: United States Geological Survey Open File Report. vol. 82, pp. 206.
- Frost, B.R., Barnes, C.G., Collins, W.J., Arculus, R.J., Ellis, D.J., Frost, C.D., 2001. A geochemical classification of granitic rocks. *J. Petrol.* 42, 2033–2048.
- Gabriele, P., 2002. HP Terranes Exhumation in an Active Margin Setting: Geology, Petrology and Geochemistry of the Raspas Complex in SW Ecuador (PhD thesis). Université de Lausanne.
- Gerya, T.V., Stöckhert, B., Perchuk, A.L., 2002. Exhumation of high-pressure metamorphic rocks in a subduction channel: a numerical simulation. *Tectonics* 21, 1056.
- Gomez, J., Nivia, A., Montes, N.E., Jimenez, D.M., Tejada, M.L., Sepulveda, J., Osorio, J.A., Gaona, T., Diederix, H., Uribe, H., Mora, M., 2007. Geological Map of Colombia. Escala 1:1'000.000, second ed. Ingeominas, Bogota.
- Gomez-Cruz, A.D.J., Moreno-Sánchez, M., Pardo, A., 1995. Edad y origen del “Complejo metasedimentario Aranzazu-Manizales” en los alrededores de Manizales (Departamento de Caldas, Colombia). In: *Geología Colombiana*. vol. 19, pp. 83–93.
- Gonzalez, H., 1980. Geología de las Planchas 167 (Sonson) e 187 (Salamina). *Bol. Geol. Ingeominas, Informe* 1760.
- Gradstein, F.M., Ogg, J.G., Smith, A.G., et al., 2004. *A Geological Timescale 2004*. Cambridge University Press, Cambridge. (39 co-authors).
- Hastie, A.R., Kerr, A.C., Pearce, J.A., Mitchell, S.F., 2007. Classification of altered volcanic island arc rocks using immobile trace elements: development of the Th-Co discrimination diagram. *J. Petrol.* 48, 2341–2357.
- Herbert, H.J., Pichler, H., 1983. K-Ar ages of rocks from the Eastern Cordillera of Ecuador. *Z. Dtsch. Geol. Ges.* 134, 483–493.

- Ingeominas, 2007a. Geologic Map of the Sierra Nevada de Santa Marta, scale 1:200.000. Ingeominas–Invemar-Ecopetrol-ICP-Geosearch. Ltda.
- Ingeominas, 2007b. Geología de las planchas 11, 12, 13, 14, 18, 19, 20, 21, 25, 26, 27, 33 Y 34. Proyecto “Evolución Geohistórica de la Sierra Nevada de Santa Marta”. Ingeominas–Invemar-Ecopetrol-ICP-Geosearch. Ltda, p. 333.
- Jaillard, E., Soler, P., Carlier, G., Mourier, T., 1990. Geodynamic evolution of the northern and central Andes during early to middle Mesozoic times: a Tethyan model. *J. Geol. Soc.* 147, 1009–1022.
- Jaramillo, J.S., Cardona, A., Leon, S., Valencia, V., Vinasco, C., 2017. Geochemistry and geochronology from Cretaceous magmatic and sedimentary rocks at 6°35'N, western flank of the Central Cordillera (Colombian Andes): magmatic record of arc growth and collision. *J. S. Am. Earth Sci.* 76, 460–481.
- John, T., Scherer, E.E., Schenk, V., Herms, P., Halama, R., Garbe-Schönberg, D., 2010. Subducted seamounts in an eclogite-facies ophiolite sequence: the Andean Raspas Complex, SW Ecuador. *Contrib. Mineral. Petrol.* 159, 265–284.
- Jolly, W.T., Lidiak, E.G., Dickin, A., Wu, T.W., 2001. Secular geochemistry of central Puerto Rican island arc lavas: constraints on Mesozoic tectonism in the eastern Greater Antilles. *J. Petrol.* 42, 2197–2214.
- Kay, S.M., Burns, W.M., Copeland, P., Mancilla, O., 2006. Upper Cretaceous to Holocene magmatism and evidence for transient Miocene shallowing of the Andean subduction zone under the northern Neuquén Basin. In: Kay, S.M., Ramos, V.A. (Eds.), *Evolution of an Andean Margin: A Tectonic and Magmatic View from the Andes to the Neuquén Basin (35°–39°S lat)*. vol. 407, pp. 19–59. Geological Society of America Special Paper.
- Kennan, L., Pindell, J., 2009. Dextral shear, terrane accretion and basin formation in the Northern Andes: best explained by interaction with a Pacific-derived Caribbean Plate? *Geol. Soc. Lond. Spec. Publ.* 328, 487–531.
- Leal-Mejia, H., Draper, J.C.M.I., Shaw, R.P., 2011. Phanerozoic gold metallogeny in the Colombian Andes. In: *Proceedings Let's Talk Ore Deposits, SGA Biennial Meeting, Antofagasta, Chile*.
- Leal-Mejía, H., Shaw, R.P., Draper, J.C.M.I., 2018. Spatial-temporal migration of granitoid magmatism and the phanerozoic tectono-magmatic evolution of the Colombian Andes. In: Cediel, F., Shaw, R.P. (Eds.), *Geology and Tectonics of Northwestern South America. Frontiers in Earth Sciences*, [https://doi.org/10.1007/978-3-319-76132-9\\_5](https://doi.org/10.1007/978-3-319-76132-9_5).
- Litherland, M., Aspden, J.A., Jemielita, R.A., 1994. The metamorphic belts of Ecuador. In: *Overseas Memoir of the British Geological Survey 11*, Nottingham, England, pp. 147.
- Luzieux, L.D.A., Heller, F., Spikings, R., Vallejo, C.F., Winkler, W., 2006. Origin and Cretaceous tectonic history of the coastal Ecuadorian forearc between 1°N and 3°S: paleomagnetic, radiometric and fossil evidence. *Earth Planet. Sci. Lett.* 249, 400–414.
- Maniar, P.D., Piccoli, P.M., 1989. Tectonic discrimination of granitoids. *Geol. Soc. Am. Bull.* 101, 635–643.
- Mantilla Figueroa, L.C., Bissig, T., Valencia, V., Hart, C.J.R., 2013. The magmatic history of the Vetas-California mining district, Santander Massif, Eastern Cordillera, Colombia. *J. S. Am. Earth Sci.* 45, 235–249.
- Maresch, W.V., Kluge, R., Baumann, A., Pindell, J.L., Krückhans-Lueder, G., Stanek, K., 2009. The occurrence of high-pressure metamorphism on Margarita Island, Venezuela: a constraint on Caribbean-South America interaction. *Geol. Soc. Lond. Spec. Publ.* 328, 705–741.
- Martin-Gombojav, N., Winkler, W., 2008. Recycling of Proterozoic crust in the Andean Amazon foreland of Ecuador: implications for orogenic development of the Northern Andes. *Terra Nova* 20, 22–31.
- Maya, M., González, H., 1995. Unidades Litodémicas en la Cordillera Central de Colombia. Informe Unidad Operativa Medellín, Ingeominas, Colombia, pp. 44–57.
- Megard, F., 1984. The Andean orogenic period and its major structures in central and northern Peru. *J. Geol. Soc. Lond.* 141, 893–900.
- Miskovic, A., Spikings, R.A., Chew, D.M., Košler, J., Ulianov, A., Schaltegger, U., 2009. Tectonomagmatic evolution of Western Amazonia: geochemical characterization and zircon U-Pb geochronologic constraints from the Peruvian Eastern Cordilleran granitoids. *Geol. Soc. Am. Bull.* 121, 1298–1324.

- Mora, A., Parra, M., Strecker, M.R., Kammer, A., Dimaté, C., Rodriguez, F., 2006. Cenozoic contractional reactivation of Mesozoic extensional structures in the Eastern Cordillera of Colombia. *Tectonics* 25, <https://doi.org/10.1029/2005TC001854>.
- Mora, A., Parra, M., Strecker, M.R., Sobel, E.R., Hooghiemstra, H., Torres, V., Jaramillo, J.V., 2008. Climatic forcing of asymmetric orogenic evolution in the Eastern Cordillera of Colombia. *Geol. Soc. Am. Bull.* 120, 930–949.
- Mora, A., Gaona, T., Kley, J., Montoya, D., Parra, M., Quiroz, Q.I., Reyes, G., Strecker, M.R., 2009. The role of inherited fault segmentation and linkage in contractional orogenesis: a reconstruction of Lower Cretaceous rift basins in the Eastern Cordillera of Colombia. *Basin Res.* 21, 111–137.
- Nivia, A., Marriner, G.F., Kerr, A.C., Tarney, J., 2006. The Quebradagrande Complex: A Lower Cretaceous ensialic marginal basin in the Central Cordillera of the Colombian Andes. *J. S. Am. Earth Sci.* 21, 423–436.
- Ordonez, M., Jiménez, N., Suárez, J., 2006. Micropaleontología Ecuatoriana. Petroproducción634.
- Orrego, A., Restrepo, J.J., Toussaint, J.F., Linares, E., 1980. Datación de un esquisto sericitico de Jambaló, Cauca. vol. 25. Geología Universidad Nacional, pp. 133–134. Special Publications.
- Paul, A.N., Spikings, R.A., Ulianov, A., Ovtcharova, M., 2018. High temperature ( $>350^{\circ}\text{C}$ ) thermal histories of the long lived ( $>500$  Ma) active margin of Ecuador and Colombia: apatite, titanite and rutile U-Pb thermochronology. *Geochim. Cosmochim. Acta* 228, 275–300.
- Peacock, M.A., 1931. Classification of igneous rock series. *J. Geol.* 39, 54–67.
- Pindell, J.L., Kennan, L., 2009. Tectonic evolution of the Gulf of Mexico, Caribbean and northern South America in the mantle reference frame: an update. *Geol. Soc. Lond. Spec. Publ.* 328, 1–55.
- Pindell, J.L., Kennan, L., Maresch, W.V., Stanek, K.P., Draper, G., Higgs, R., 2005. Plate kinematics and crustal dynamics of circum-Caribbean arc-continent interactions: tectonic controls on basin development in Proto-Caribbean margins. In: Lallemand, A., Sisson, V.B. (Eds.), Caribbean-South American Plate Interactions. vol. 394. Geological Society of America, pp. 7–52. Special Paper.
- Piraquive, B.A., 2017. Structural framework, deformation and exhumation of the Santa Marta Schists: accretion and deformational history of a Caribbean Terrane at the north of the Sierra Nevada de Santa Marta. PhD Thesis Universidad Nacional de Colombia, Bogota, pp. 262.
- Pratt, W.T., Duque, P., Ponce, M., 2005. An autochthonous geological model for the eastern Andes of Ecuador. *Tectonophysics* 399, 251–278.
- Rapela, C.W., Pankhurst, R.J., Fanning, C.M., Herve, F., 2005. Pacific subduction coeval with the Karoo mantle plume: the early Jurassic subcordilleran belt of northwestern Patagonia. In: Vaughan, A.P.M., Leat, P.T., Pankhurst, R.J. (Eds.), Terrane Processes at the Margins of Gondwana. Geological Society of London, pp. 217–239. Geological Society Special Publications, 246.
- Restrepo, J.J., Toussaint, J.F., 1976. Edades radiométricas de algunas rocas de Antioquia. vol. 12. Publicación Especial Geología. Universidad Nacional de Medellín, Colombia, pp. 1–11.
- Restrepo, J.J., Ordóñez-Carmona, O., Moreno-Sánchez, M., 2009. A comment on “The Quebradagrande Complex: a Lower Cretaceous ensialic marginal basin in the Central Cordillera of the Colombian Andes” by Nivia et al. *J. S. Am. Earth Sci.* 28, 204–205.
- Riding, J.B., 1989. A Palynological Investigation of Nine Rock Samples from Ecuador (Maguazo Unit). . British Geological Survey Technical Report WH/89/361/R, 4 pp.
- Rodríguez, G., Zapata, G., 2013. Comparative analysis of the Barroso formation and Quebradagrande complex: a volcanic arc tholeiitic-calcoalcaline, segmented by the fault system Romeral in Northern Andes. *Bol. Cienc. Tierra* 33, 39–58.
- Rodríguez, G., Arrango, M.I., Zapata, G., Bermúdez, J.G., 2018. Petrotectonic characteristics, geochemistry, and U-Pb geochronology of Jurassic plutons in the Upper Magdalena Valley-Colombia: implications on the evolution of magmatic arcs in the NW Andes. *J. S. Am. Earth Sci.* 81, 10–30.
- Romero, C.W.C., 2018. Identificación y Caracterización de Facies de la Formación Hollín en Centro Shaime: El Registro de una Transición Fluvio-Marina en la Región Sur Oriental del Ecuador. (Ing thesis) Escuela Politécnica National, Quito, p. 214.

- Romeuf, N., Aguirre, L., Soler, P., Féraud, G., Jaillard, E., Ruffet, G., 1995. Middle Jurassic volcanism in the Northern and Central Andes. *Rev. Geol. Chile* 22, 245–259.
- Ruiz, G.M.H., Seward, D., Winkler, W., 2004. Detrital thermochronology: a new perspective on hinterland tectonics, an example from the Andean Amazon Basin, Ecuador. *Basin Res.* 16, 413–430.
- Ruiz, G., Seward, D., Winkler, W., Maria, A.M., David, T.W., 2007. Evolution of the Amazon Basin in Ecuador with special reference to hinterland tectonics: data from zircon fission-track and heavy mineral analysis. *Dev. Sedimentol.* 58, 907–934.
- Sarmiento, L.F., Rangel, A., 2004. Petroleum systems of the Upper Magdalena Valley, Colombia. *Mar. Pet. Geol.* 21, 373–391.
- Sarmiento-Rojas, L.F., Van Wess, J.D., Cloetingh, S., 2006. Mesozoic transtensional basin history of the Eastern Cordillera, Colombian Andes: inferences from tectonic models. *J. S. Am. Earth Sci.* 21, 383–411.
- Scheuber, E., González, G., 1999. Tectonics of the Jurassic–Early Cretaceous magmatic arc of the north Chilean Coastal Cordillera (22°–26°S): a story of crustal deformation along a convergent plate boundary. *Tectonics* 18, 895–910.
- Sempere, T., Carlier, G., Soler, P., Fornari, M., Carlotto, V., Jacay, J., Arispe, O., Néraudeau, D., Cárdenas, J., Rosas, S., Jiménez, N., 2002. Late Permian–Middle Jurassic lithospheric thinning in Peru and Bolivia, and its bearing on Andean-age tectonics. *Tectonophysics* 345, 153–181.
- Spikings, R.A., Crowhurst, P.V., Winkler, W., Villagomez, D., 2010. Syn- and post accretionary cooling history of the Ecuadorian Andes constrained by their in-situ and detrital thermochronometric record. *J. S. Am. Earth Sci.* 30, 121–133.
- Spikings, R., Cochrane, R., Villagómez, D., Van der Lelij, R., Vallejo, C., Winkler, W., Beate, B., 2015. The geological history of northwestern South America: from Pangaea to the early collision of the Caribbean Large Igneous Province (290 – 75 Ma). *Gondwana Res.* 27, 95–139.
- Sun, S.S., McDonough, W.F., 1989. Chemical and isotopic systematics of oceanic basalts: implications for mantle composition and processes. *Geol. Soc. Lond. Spec. Publ.* 42, 313–345.
- Teson, E., Mora, A., Silva, A., Namson, J., Teixell, A., Castellanos, J., Casallas, W., Julivert, M., Taylor, M., Ibañez-Mejía, M., Valencia, V.A., 2013. Relationship of Mesozoic graben development, stress, shortening magnitude, and structural style in the Eastern Cordillera of the Colombian Andes. *Geol. Soc. Lond. Spec. Publ.* 377, <https://doi.org/10.1144/SP377.10>.
- Toussaint, J.F., Restrepo, J.J., 1994. The Colombian Andes during Cretaceous times. In: Salfity, J.A. (Ed.), *Cretaceous Tectonics of the Andes*. Earth Evolution Series, Vieweg and Teubner Verlag, pp. 61–100.
- Toussaint, J.F., Gonzalez, H., Restrepo, J., Linares, E., 1978. Edad K/Ar de tres rocas metamórficas del flanco noroccidental de la Cordillera Central. Publicación Especial Geológica N° 14. Facultad de Ciencias, Medellín, p. 7.
- Tschanz, C.M., Marvin, R.F., Cruz, J., Mehnert, B.H.H., Cebula, G.T., 1974. Geologic evolution of the Sierra Nevada de Santa Marta, Northeastern Colombia. *Geol. Soc. Am. Bull.* 8, 273–284.
- Vallejo, C., Spikings, R.A., Luzieux, L., Winkler, W., Chew, D., Page, L., 2006. The early interaction between the Caribbean Plateau and the NW South American Plate. *Terra Nova* 18, 264–269.
- Van der Lelij, R., Spikings, R., Ulianov, A., Chiaradia, M., Mora, A., 2016. Palaeozoic to Early Jurassic history of the northwestern corner of Gondwana, and implications for the evolution of the Iapetus, Rheic and Pacific Oceans. *Gondwana Res.* 31, 271–294.
- Vasquez, M., Altenberger, U., 2005. Mid-Cretaceous extension-related magmatism in the eastern Colombian Andes. *J. S. Am. Earth Sci.* 20, 193–210.
- Vasquez, M., Altenberger, U., Romer, R.L., Sudo, M., Moreno-Murillo, J.M., 2010. Magmatic evolution of the Andean Eastern Cordillera of Colombia during the Cretaceous: influence of previous tectonic processes. *J. S. Am. Earth Sci.* 29, 171–186.
- Vergara, L., Prössl, K.F., 1994. Dating the Yaví Formation (Aptian, Upper Magdalena Valley, Colombia), palynological results. In: Etayo, F. (Ed.), *Estudios Geológicos del Valle Superior del Magdalena*. Bogotá, Departamento de Geociencias, Universidad Nacional de Colombia, pp. 14.

- Villagomez, D., Spikings, R., 2013. Thermochronology and tectonics of the Central and Western Cordilleras of Colombia: Early Cretaceous–Tertiary evolution of the Northern Andes. *Lithos* 168, 228–249.
- Villagomez, D., Spikings, R., Magna, T., Kammer, A., Winkler, W., Beltrán, A., 2011. Geochronology, geochemistry and tectonic evolution of the Western and Central cordilleras of Colombia. *Lithos* 125, 875–896.
- Vinasco, C.J., Cordani, U.G., González, H., Weber, M., Pelaez, C., 2006. Geochronological, isotopic, and geochemical data from Permo-Triassic granitic gneisses and granitoids of the Colombian Central Andes. *J. S. Am. Earth Sci.* 21, 355–371.

---

## Further reading

- Kuiper, K.F., Deino, A., Hilgen, F.J., Krijgsman, W., Renne, P.R., Wijbrans, J.R., 2008. Synchronising rock clocks of earth history. *Science* 25, 500–504.